US Army Corps of Engineers
Construction Engineering Research Laboratories

CERL Technical Report 99/05
December 1998

Removal and Recovery of Organic Vapor Emissions by Fixed-Bed Activated Carbon Fiber Adsorber–Cryogenic Condenser

by
Mark J. Rood
Mehrdad Lordgooei
Chloe S. Reece
Shaoying Qi
K. James Hay

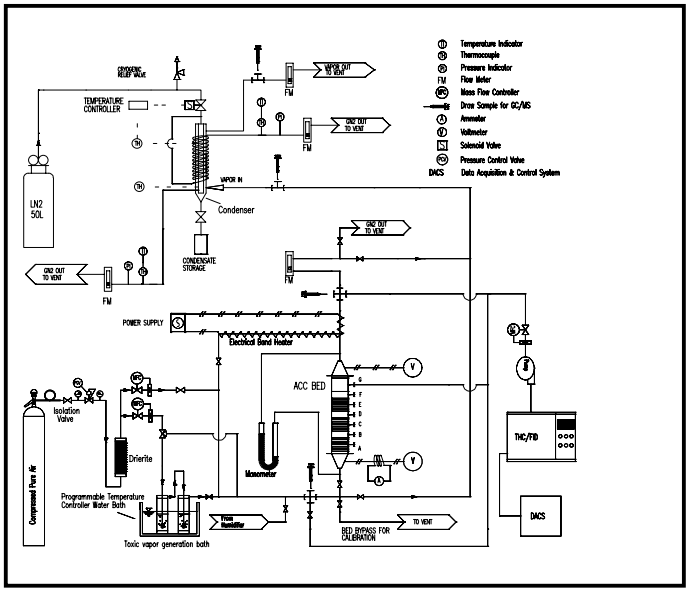

Abatement of toxic volatile organic compounds (TVOCs) emitted to the atmosphere has become a concern because of the magnitude of the emissions and their potential health effects to humans and deleterious effects to the environment. New control technologies are being developed to separate and remove those toxic compounds from gas streams for reuse of the TVOCs in the process that generated them. This project evaluated the ability of an activated carbon fiber cloth (ACFC) adsorption, electrothermal desorption, cryogenic-condensation system to remove 10 cm^3/min containing 1000 ppmv of methyl ethyl ketone (MEK) or toluene from air streams that are dry or at 90 percent relative humidity. Results indicate that MEK and toluene are readily adsorbed from the carrier gas streams with the ACFC adsorber. Electrothermal desorption is also effective at desorbing the TVOCs and water from the ACFC. Cryogenic condensation is also effective for the dry MEK and toluene desorption conditions.

Foreword

This study was conducted for Headquarters, U.S. Army Corps of Engineers (HQUSACE) under Project 4A162720DO48, "Industrial Operations Pollution Control Technology"; Work Unit T87, "Strategies for Minimizing Hazardous Air Pollutants from Industrial Operations."

The study was primarily performed by the Industrial Operation Division (UL-I) of the Utilities and Industrial Operations Laboratory (UL), U.S. Army Construction Engineering Research Laboratories (CERL). The CERL principle investigator is Dr. K. James Hay. Dr. Shaoying Qi is a contractor under the IPA with the University of Cincinnati, Cincinnati, OH. Dr. Mark J. Rood is an associate professor in the Department of Civil Engineering at the University of Illinois, Urbana-Champaign, IL. Mehrdad Lordgooei and Chloe S. Reece are research assistants with the University of Illinois at Urbana-Champaign. Walter J. Mikucki was Chief, CERL-UL-I; Dr. John T. Bandy was Operations Chief, CERL-UL; and Gary W. Schanche was the responsible technical Director, CERL-TD. The CERL technical editor was William J. Wolfe, Technical Resources.

Dr. Michael J. O'Connor is Director of CERL.

Contents

List of Figures and Tables

Figures

Tables

1 Introduction

Background

Toxic Releases to the Environment

Abatement of toxic pollutants has gained recent attention due to a better understanding of the effects of releasing these compounds into the environment. The magnitude of the emissions and their hazards have led to public health concern and recent government regulations to reduce the amount of their emissions to the environment.

The U.S. Environmental Protection Agency (USEPA) began compiling a database of toxic-pollutant releases into the environment in all 50 States and U.S. jurisdictions in 1987. Facilities manufacturing or processing 11,340 kg/yr of toxic materials and/or 4,500 kg/yr of "other use" toxic materials (e.g., solvents, cleaning materials, etc.) are required to report their toxic releases into the environment to the USEPA (1993a). Data reported for 1993 indicated that 1.7 x 10^9 kg/yr of toxic pollutants were emitted to the atmosphere in the United States (USEPA 1995). This data included information about 316 toxic chemicals and 20 categories of chemical compounds. The original selection of compounds was first compiled from lists established by the States of Maryland and New Jersey for State toxic reporting. These compounds have been identified as "posing a risk to human health or the environment." The list of 316 toxic chemicals is under continual public, USEPA, and U.S. Congressional review for alterations.

From the list of toxic emissions, USEPA has identified 189 hazardous air pollutants (HAPs) for Federal regulation (USEPA 1990). Selection of many of the HAPs listed in Section 112 of the 1990 Clean Air Act Amendments (CAAAs) was based on the compounds' "potential to cause increased mortality or serious illness." For example, many of these toxic pollutants are known to be human carcinogens (USEPA 1993a). Exposure is also known or suspected to cause many other noncancer effects, including poisoning, immunological, neurological, reproductive, developmental, mutagenic, and respiratory problems (Burge and Hodgson 1988). Risk assessment of exposure to toxic air pollutants is difficult for effects related to cancer, and much more difficult for noncancer effects due to

the many different possible exposure effects (USEPA 1993a). USEPA is required under the 1990 CAAAs to evaluate residual risk remaining after the implementation of technology-based standards.

Many HAPs can be further classified as TVOCs. In general, USEPA categorizes volatile organic compounds (VOCs) as low, moderate, and high volatility based on the compound's vapor pressure at 293 K. Compounds with a vapor pressure less than 0.01 MPa at 293 K, including toluene, are classified in the low volatility category. Compounds with a vapor pressure between 0.01 and 0.02 MPa, including methyl ethyl ketone (MEK) are in the moderate volatility category. Atmospheric emissions of TVOCs appearing on the USEPA's list of HAPs totaled 4.5×10^8 kg for 1991 (USEPA 1993a). In addition, of the 10 HAPs with the highest emission rates in that year, eight were TVOCs, and these eight accounted for ~95 percent of the total TVOC emissions. In 1993, toluene ranked highest on the TRI list of chemicals with the 10 largest emission rates to the air, with 8×10^7 kg/yr of toluene emitted, and MEK had the seventh largest emission rate of 3.9×10^7 kg/yr (USEPA 1995). Toluene and MEK accounted for 10 and 5 percent of the TRI releases to the air, respectively. Table 1 lists properties of toluene and MEK.

In general, VOC emissions to the atmosphere have declined from 1987 to 1991 by approximately 5 percent/yr (USEPA 1993a). This is primarily due to government regulation of VOC emissions (McIlvaine et al. 1993). Under the USEPA proposed Hazardous Organic National Emissions Standards for Hazardous Air Pollutants (HON) rule, 370 chemical manufacturing facilities and 1,050 chemical manufacturing processes will be required to reduce emissions of TVOC from 5.6×10^8 kg/yr in 1989 to 1.1×10^8 kg/yr by 1998 (USEPA 1993a). Because of the amount of HAPs emitted to the atmosphere each year by U.S. Army industrial facilities, U.S. Army operations may also be subject to technology-based emission standards, and will be required to comply with these standards within 3 years of their promulgation.

In addition to their adverse health effects, many TVOCs are also known to be ozone precursors. Ozone can cause eye, nose, throat, and respiratory problems in humans, especially in urban areas (Tolley et al. 1993). This is in part the reason for the mandated reduction of VOCs under Title I in ozone nonattainment areas (USEPA 1990).

Table 1. Properties of methyl ethyl ketone (MEK) and toluene.

Property Name (units)	Methyl Ethyl Ketone (MEK)	Toluene
Molecular Formula	C_4H_8O	$C_6H_5CH_3$
Molecular Weight (g/gmol)	72.1	92.1
Density @ 20°C (g/cm^3)	0.805	0.866
Saturation Vapor Pressure (mmHg)	89.5	28.34
Boiling Point (°C)	79.6	110.6
Solubility (g in 100g H_2O)	35 (@ 10°C)	0.05 (@ 16°C)
Surface Tension @ 20°C (dyne/cm)	24.6	28.5
Dipole Moment (debyes)	3.2	0.45
**Sources: M.P. Cal (1995); Y. Marcus (1992); R.H. Perry and C.H. Chilton (1973)		

Federal Air Quality Regulations

Between 1970 and 1990, the USEPA regulated eight HAPs (i.e., arsenic, asbestos, benzene, beryllium, mercury, radio nuclides, radon-222, and vinyl chloride) under the National Emission Standards for Hazardous Air Pollutants (NESHAPS). During this time, however, CAAAs of 1977 were updated, and these new amendments were signed into law in 1990. As a result of this 1990 legislation, USEPA is required to establish technology-based guidelines for the reduction of TVOC emissions to the atmosphere from point sources (USEPA 1990). Specifically, control based reduction of VOCs falls under Title I and Title III of the 1990 CAAAs. Effectively, VOC emissions in ozone nonattainment areas are governed by Title I, and TVOCs are governed by Title I and Title III.

Under Title I of the 1990 CAAAs, the USEPA is required to establish reasonable achievable control technology (RACT) standards for point source VOC emissions in ozone-related nonattainment areas. State environmental regulatory agencies are responsible for implementation of RACT standards. RACT is defined as “the lowest emission limitation that a particular source is capable of meeting by the application of control technology that is reasonably available considering technological and economic feasibility” (USEPA 1991). A compilation of information was developed for State use in determining State-specific RACT implementation. For example, USEPA developed an information base on VOC emissions of 17 categories of industries (USEPA 1993), control technology techniques, and cost of implementation of various control technologies (USEPA 1991).

Title III of the 1990 CAAAs requires the USEPA to establish maximum achievable control technology (MACT) standards for point source emissions of HAPs. MACT standards are based on the best demonstrated control technology

and/or practices and are not dependent on the cost of the technology. These standards apply to all major sources with the potential to emit at least 10 tons/yr of any one of the HAPs, or at least 25 ton/yr of any combination of HAPs. Area sources are also subject to MACT standards. HAP emission standards for point sources based on MACT should be promulgated by 15 November 2000. Furthermore, sources regulated under Title III must meet permit requirements within 3 yr of promulgation (USEPA 1991). U.S. Army industrial operations will need to comply with these MACT standards on the same 3-yr schedule as other regulated sources.

Addressing the Air Pollution Control Requirements

Existing sources of air pollution will spend $19.4 billion to meet Title I and Title III requirements of the 1990 CAAAs (McIlvaine 1993). Of the $19.4 billion, direct expenditures on air pollution control equipment are estimated at $6.5 billion. The development of new control equipment is at least in part necessitated by the requirements to remove TVOCs from point source emissions. Because of the size of this investment, there is interest in developing efficient means of removing TVOCs from gas streams for reuse.

Point source TVOC emission reduction is generally accomplished by: (1) process modification, (2) feed stream modification, (3) source shutdown, and/or (4) utilization of ancillary control devices. While process modification is generally the most economical method of reducing TVOC emissions, further reduction of these emissions beyond what is achievable through modification usually requires the addition of control devices to treat the waste stream (Ruddy and Carrol 1993).

The most widely used control devices that remove VOCs from gas streams are: (1) thermal incinerators, (2) catalytic incinerators, (3) flares, (4) boilers/process heaters, (5) adsorbers, (6) absorbers, and (7) condensers (USEPA 1991). Due to the focus of the present research, descriptions for most of these will be omitted in this report. Only the basic principles of carbon adsorbers and condensers are relevant to this investigation.

Adsorption systems capture TVOCs at the adsorbent's internal and external surface areas. Activated carbon is the most widely used adsorbent for VOC removal (USEPA 1991; Noll et al. 1992). Typically the adsorbent is regenerated either thermally at an elevated temperature (typically with steam) or under a vacuum.

Condensers can be used to remove VOCs from gas streams by lowering the temperature of the stream below the saturation temperature of the VOC. The gaseous VOC changes phase from a gas to liquid at the saturation temperature and thus the contaminant would be removed from the gas stream. Recovery of VOCs by condensation should be considered when a relatively pure condensate with a monetary value greater than $0.66/kg can be recovered (Dyer and Mulholland 1994).

In this research, an activated carbon fiber cloth (ACFC) adsorption system was designed, developed, and characterized for possible use as a method for point source reduction of toluene and MEK emissions. In the developed system, ACFC adsorption is followed by electrothermal regeneration resulting in formation of a concentrated organic vapor that may be cryogenically condensed from the gas phase. A bench-scale cryogenic condenser was used to assess the fundamental performance of condensing TVOCs at low temperatures.

Objectives

The objectives of this research were to assess the process efficiency and to obtain design and operation parameters for the fixed-bed ACFC adsorber, coupled with a cryogenic condenser, for removal and recovery of MEK and toluene from vapor emissions.

Approach

This report describes the development and laboratory evaluation of an ACFC adsorption system that has been integrated with electrothermal desorption and liquid N_2 (LN_2) cryogenic condensation. The intent of this new technology is to: (1) reduce the amount of MEK and toluene emitted to the atmosphere, (2) meet MACT standards, and (3) provide for reuse of the TVOCs that are recovered. In the adsorber, TVOCs are selectively separated from influent gas stream by the attraction force fields generated from micropore wells in the ACFC fibers. ACFC adsorption is followed by electrothermal regeneration, resulting in formation of a concentrated organic vapor. The concentrated TVOC is then condensed using LN_2 as the refrigerant. LN_2 can reduce TVOC emission concentrations to parts ber billion be volume (ppbv) concentrations due to its high latent heat of vaporization. This integrated system can enable sources of TVOCs such as MEK and toluene to meet air quality control regulations while providing a high quality liquid product for reuse.

Development and testing of this integrated system for the compounds of interest was achieved through the completion of three specific tasks:

1. The first task required developing the set-up for the experimental apparatus. The system consisted of a gas generation system, the ACFC fixed-bed adsorber, electrothermal regenerator, the cryogenic condenser, a gas detection system, and a data acquisition and control system (DACS). Details of each of these components are provided in Chapter 2.
2. The next task involved performing experiments and using their results to assess the process efficiency of the ACFC adsorption system and to obtain design and operation parameters. In total, 12 adsorption/desorption cycles were performed, providing triplicate results for each of four sets of inlet gas stream conditions. Tests were performed for toluene and MEK at concentrations of ≈ 1,000 parts per million by volume (ppmv) in dry air and in air with a relative humidity (RH) ≈ 90 percent.
3. The final task resulted in an assessment of the integrated ACFC adsorber-cryogenic condenser system, including recommendations regarding the viability of using this pollution control technology for toluene and MEK emission removal and recovery at U.S. Army facilities. Suggestions were also developed for any design changes or optimization needs that might be required before the system could be tested at the pilot-reactor scale.

2 Experimental System

Overall System Design

Figure 1 shows the laboratory-scale ACFC adsorption-cryogenic vapor recovery system. The integrated system is composed of gas generator, ACFC fixed bed adsorber, regenerator, cryogenic condenser, analytical measurement instruments, and DACS. The calibrated gas stream passes through the fixed bed of ACFC, where the organic material is separated from the carrier gas by adsorption. The exhaust gas from the fixed-bed is analyzed continuously for the concentration of TVOC. The exhaust gas is vented under a hood.

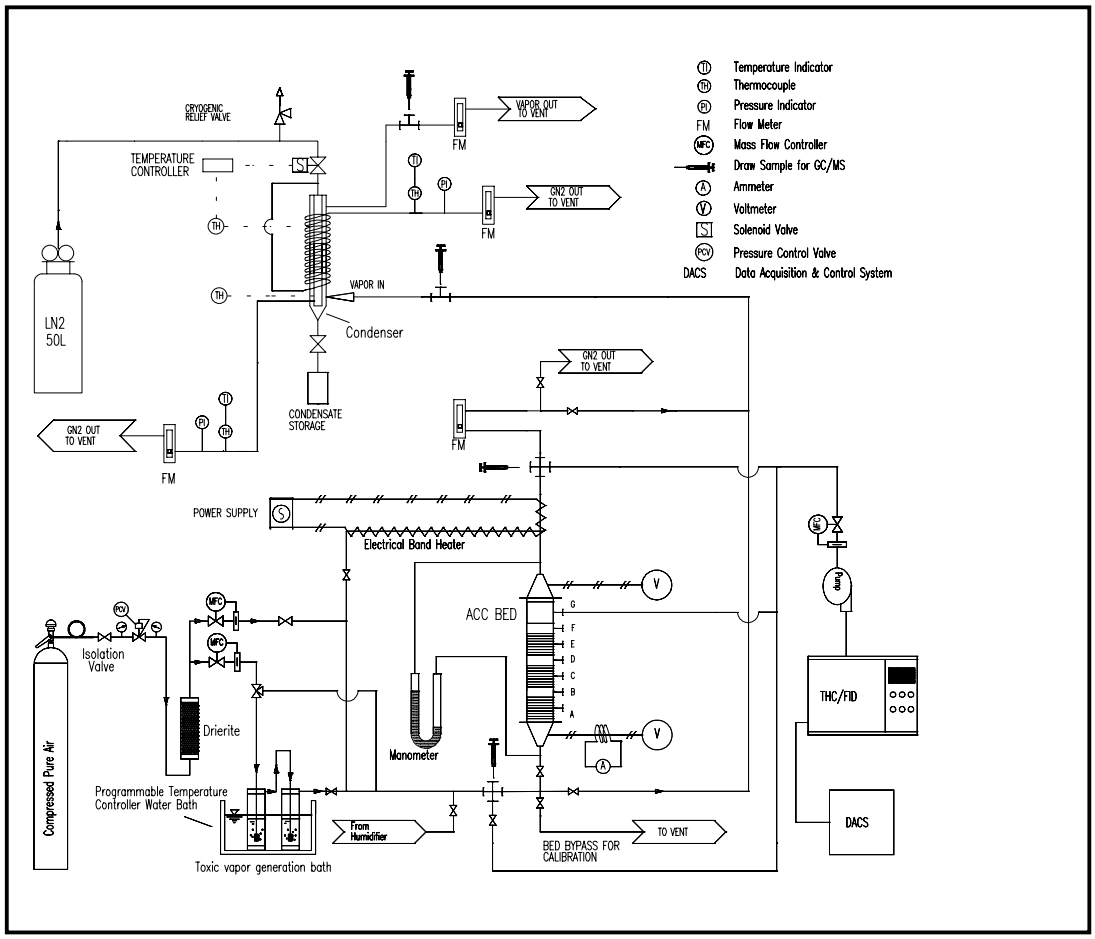

Figure 1. Laboratory-scale ACFC adsorption-cryogenic recovery system.

After saturation of the ACFC with TVOC, pure N_2 gas is passed through the adsorption bed, and electrical power is supplied to the ACFC. Electrothermal energy regenerates the adsorption capacity of the ACFC and provides an N_2 gas stream containing the desorbed TVOC. Concentration of TVOC in the N_2 carrier gas is controlled by the electrical power applied to the ACFC and the flow rate of the carrier gas. The concentrated vapor stream is then directed to the custom-designed shell-and-tube cryogenic condenser where the TVOC is condensed on the condenser's internal cold surfaces (Lordgooei et al. 1996). The condensed TVOC is transferred from the bottom of the condenser into an Erlenmeyer flask, and the recovered product can then be analyzed for purity.

Simulated Gas Generation

The gas generation system for an adsorption run performed with TVOC in dry air is also shown in Figure 1. Air from a compressed gas cylinder passes through a purifier desiccant (Drierite, Model L68GP) where trace water and organic vapors are removed. Then the purified air is branched to two separate streams controlled by two mass flow controllers (Tylan Models FC-260 and FC-280). One air stream passes through two fritted glass bubblers connected in series and immersed in a temperature-controlled water bath (Brinkman mgw lauda, Model RC-20). The bubblers contain the specified liquid TVOC, causing the air stream to become saturated in TVOC vapor. The saturated gas stream is then mixed with the second pure air stream to produce a gas mixture with a desired TVOC concentration and total flow rate.

When testing the effect of RH on the performance of the fixed-bed, the above gas generation set-up must be modified. The dry air stream passing through the glass bubblers, which becomes saturated with TVOC vapor, remains unchanged. Air passing through the bubblers need not be humidified, since this flow is < 2 percent of the total flow through the fixed bed. The second air stream, used for diluting the TVOC saturated gas stream, is regulated by the same mass flow controller and is then passed through a custom annular humidifier, contained in a 1-in. outer diameter stainless steel tube (Figure 2) (Koloutsou-Vakakis 1996). Inside this tube, a Goretex® Teflon® membrane is supported by a cylindrical 5/8-in. inside-diameter stainless-steel wire-mesh tube. Liquid deionized water passes between the outer stainless steel tube and the membrane. The air stream passes inside the stainless steel wire mesh tube and the membrane. The membrane permits transport of water vapor, but not liquid water, into the air stream. Liquid water enters at the bottom of the humidifier and is drawn out at the top, allowing uniform flow of water along the outside of the membrane.

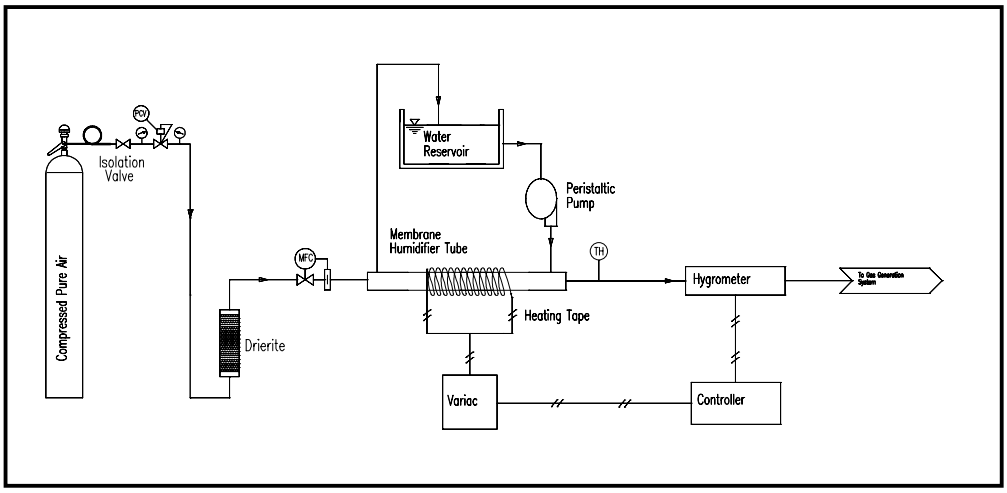

Figure 2. Gas generation humidification system.

The inlet and outlet flow rates of water are controlled with a peristaltic pump (Cole-Parmer Master Flex, Model 7518-10). Heating tape surrounds the outer stainless tube so that the temperature of the water (and the partial pressure of water vapor) can be controlled, thereby controlling the amount of water vapor passing through the membrane into the air stream.

RH of the gas stream is measured downstream of this humidifier, using a capacitive RH sensing device (Vaisala, Model HMP-233). The RH sensor is also connected to a proportional integral derivative (PID) controller (Watlow, Series 982). The desired RH setpoint is adjusted on the Watlow controller, which compares the output from the RH sensor to the defined setpoint. The PID controller can then alter the RH of the gas stream by turning on and off the AC power connected to the heating tape. This air stream, humidified to 90 percent RH, is then mixed with the TVOC-saturated air stream to create an air stream containing both water vapor and ≈ 1000 ppmv of TVOC.

Flow rates through the mass flow controllers were verified with a flow calibrator (Bios International, Dry-Cal Model DC-2). The actual concentration of the TVOC-laden gas stream was measured using the total hydrocarbon (THC) analyzer with flame ionization detector (FID), described below. The THC analyzer was calibrated using standard compressed gas cylinders from Matheson Gas, Inc. In addition, draw samples from the inlet gas stream were injected into the gas chromatograph/mass spectrometer (GC/MS, described below) throughout the adsorption tests to monitor concentration of TVOC in the gas stream sent into fixed-bed.

Adsorber

The activated carbon fiber cloth fixed-bed is 16.2 cm^2 and square in cross section, with the fiber cloth aligned normal to the flow of the TVOC-laden gas stream. The side walls of the fixed-bed are made of electrical-grade Teflon® sheets. The Teflon® is nonporous and inert, and is an electrical insulator. The temperature working range of the Teflon® sheet was provided by manufacturer to be between -195 to 260 °C.

Four pairs of 304 stainless steel frames support the pleated ACFC inside the bed, allowing up to four separate ACFC modules to be installed in the bed at one time. Each frame has 16, 1.14 mm diameter holes, spaced 3.05 mm apart along its top and bottom edges that hold 1.6 mm stainless steel rods to provide spacing between each ACFC pleat. The modules are held into place with grooves along each side of the bed, but can easily slide in and out of the bed allowing for installation of the pleated ACFC. In the modules, ACFC layers are installed in a parallel pleated crossflow fashion. This allows for flexibility in effective adsorption bed length and apparent packing density. With a 1.14 mm separation distance between each layer, the bed's apparent packing density of ACFC is 94.5 mg/cm^3. The bed's ACFC packing density can be increased to 600 mg/cm^3.

Four silicon rubber cords, placed in four shallow grooves that were machined in the intersections of the bed side walls, seal the edges of the fixed-bed against gas leakage. The side walls are externally clamped and supported with an aluminum grip arrangement consisting of four separate sections connected by bolts. Tightening the grip provides the compression stress required by the silicon rubber cords and ACFC module sides to seal the bed against gas leakage and internal channeling. Eight tension rods press two stainless steel flanged nozzles against the ends of the fixed-bed and seal those areas. Seven sampling ports, sealed with silicon rubber o-rings, were installed along the length of ACFC fixed-bed for gas sampling and temperature measurement.

The ACFC fixed-bed was fabricated by the University of Illinois at Urbana-Champaign. Figure 3 shows the fabricated bed in full and partially assembled configurations. Three 155x3.4 cm strips of ACC-5092-20 ACFC were woven into three modules. The modules were placed inside the bed and connected electrically in series. The total mass of ACFC in these three modules was 19.2 grams. Table 2 lists properties of the ACFC.

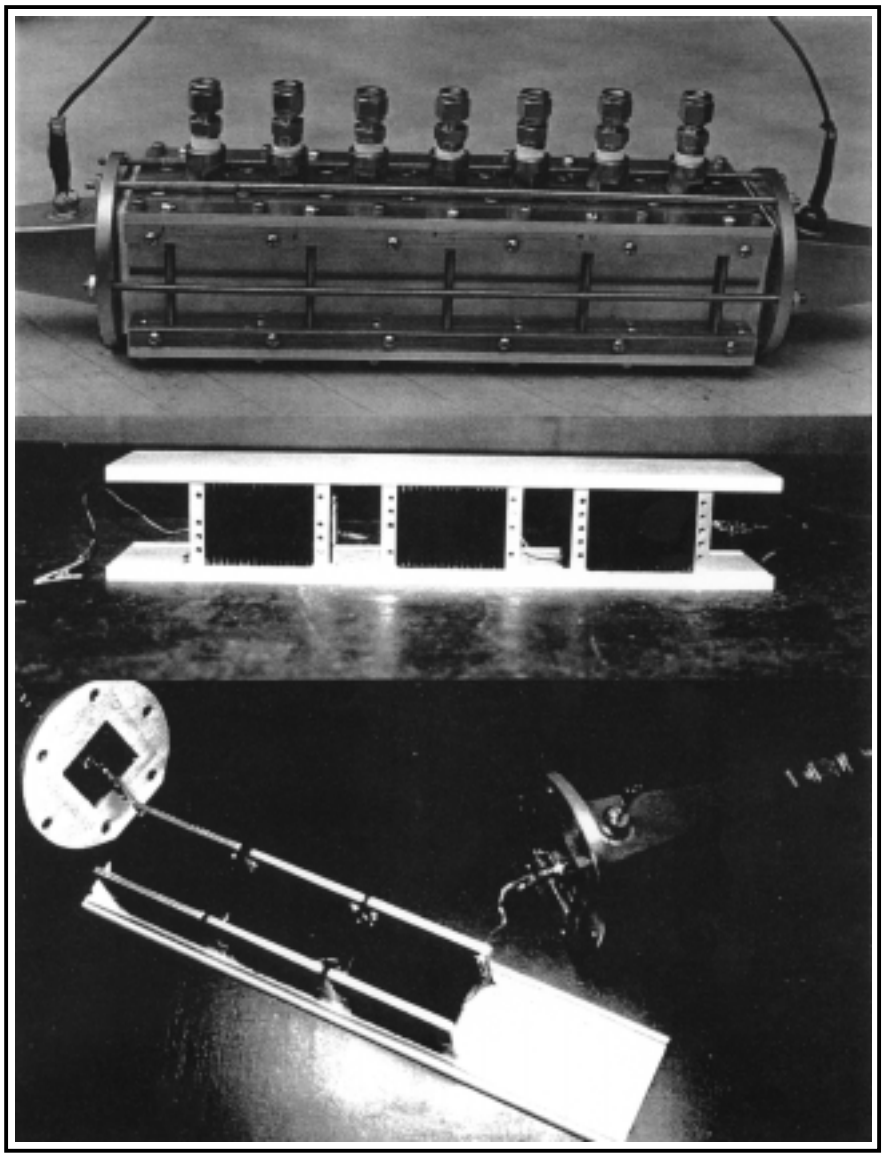

Figure 3. ACFC fixed-bed, fully and partially assembled.

Table 2. Properties of activated carbon fiber cloth.

Type	Kynol™ ACC-5092-20
Weight	150 (g/m^2)
Cloth thickness	0.55 (mm)
Fiber diameter	10-13 (m)
Weave	Modified basket 2 × 1
Construction	60 × 40 (epi x ppi)
Nominal BET specific surface area	1600 (m^2/g)
Nominal Langmuir specific surface area	2000 (m^2/g)
Single point pore volume of pores less than 396 at P/Po=0.949	0.759 (cc/g)
Micropore volume	0.690 (cc/g)
Average pore diameter (V/4A by Langmuir)	14.5 (A)
Average micropore width	6.7 (A)

During the experiments, the TVOC-laden air stream passed downward through the fixed-bed. A variable-diameter flow meter (Omega, Model FL-3439ST) was located downstream of the bed to verify that there were no leaks in the fixed bed. The gas stream exiting the adsorption bed was then sent to the THC analyzer, with excess flow to the exhaust hood.

Regenerator

Electrothermal desorption is used to regenerate the adsorption capacity of the carbon cloth adsorbent (Figure 4). Electrothermal desorption is a relatively new method of regeneration that is not yet fully used in adsorption systems. During the electrothermal regeneration process, an electric current is passed through the ACFC adsorbent. Electrical work due to phonon and defect scattering in activated carbon is directly transformed to thermal energy in the adsorbent and the adsorbed TVOC. By the flow of electric current, the thermal energy of the adsorbed molecules increases to a level that overcomes the surface bonding energy. Eventually the TVOC desorbs from the ACFC. Since electrical work is transformed directly to desorption energy, the carrier gas temperature is substantially lower than the temperature of the ACFC.

In the fixed bed, the ACFC layers are connected electrically in parallel in three separate modules. The modules are electrically connected in series. The resulting circuit is connected to a 120 V 60 Hz AC power source controlled by a variable voltage transformer (Variac) and monitored by a voltmeter and an external ammeter. This arrangement allows uniform electrical heating and careful control of the TVOC desorption process.

During regeneration, the carrier gas is switched from air to ultra high purity (UHP) N_2. This minimizes possible explosion hazards that would be present in a system containing electricity, elevated temperatures, flammable TVOCs, and oxygen. The flow rate of pure N_2 gas that passed through the adsorption bed was $\leq$ 20 percent of the total gas flow rate during adsorption. Because of the low carrier gas flow rate, the gas stream leaving the fixed bed during regeneration can contain high concentrations of toluene or MEK. During the initial phases of desorption, when these concentrations are highest, it was necessary to dilute the gas stream exiting the bed with a known amount of additional UHP N_2 before sending the desorption gas stream to the THC, due to the instrument's upper limit of detection.

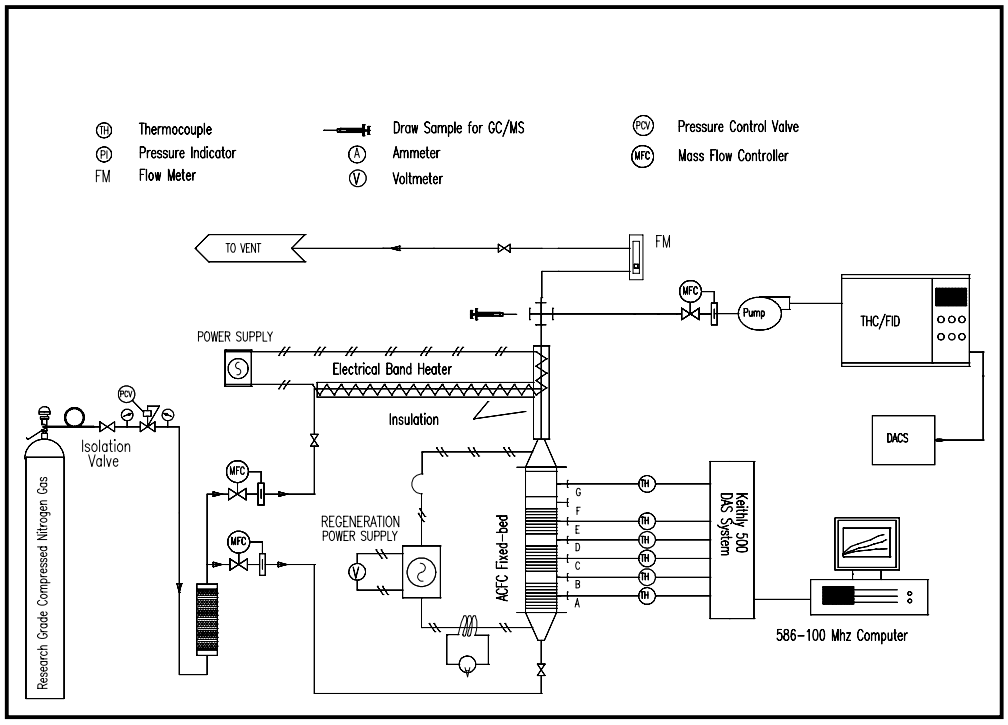

Figure 4. Schematic of electrothermal regeneration set-up.

Condensation Unit

The concentrated TVOC-N_2 gas stream exiting the bed during regeneration is sent directly to a shell-and-tube counter-current cryogenic condenser (Figure 5) (Carmichael 1996). Desorbed TVOC in the N_2 carrier gas is sent through the insulated shell. LN_2 is used as the tube side refrigerant to cool the condenser to temperatures near the freezing point of the TVOC. Although condensers can be operated with other refrigerants, LN_2 is used due to its cooling capacity, low achievable temperatures, and possible re-use capabilities. In addition to its main path in the tube side of the condenser, LN_2 is also circulated through an 1/8-in. outer diameter copper tube coil jacket wound around the outside shell of the condenser. A second temperature gradient is thus established. The temperature gradients draw heat from the vapor laden gas stream and form concentration gradients in which the organic diffuses from the bulk flow into the condensate film at the condenser walls. Because of the LN_2 flow on both sides of the shell, TVOC could condense on both of its inner walls, thereby increasing the efficiency of the recovery process. The condensed TVOC film is continually drained from the condenser by gravity.

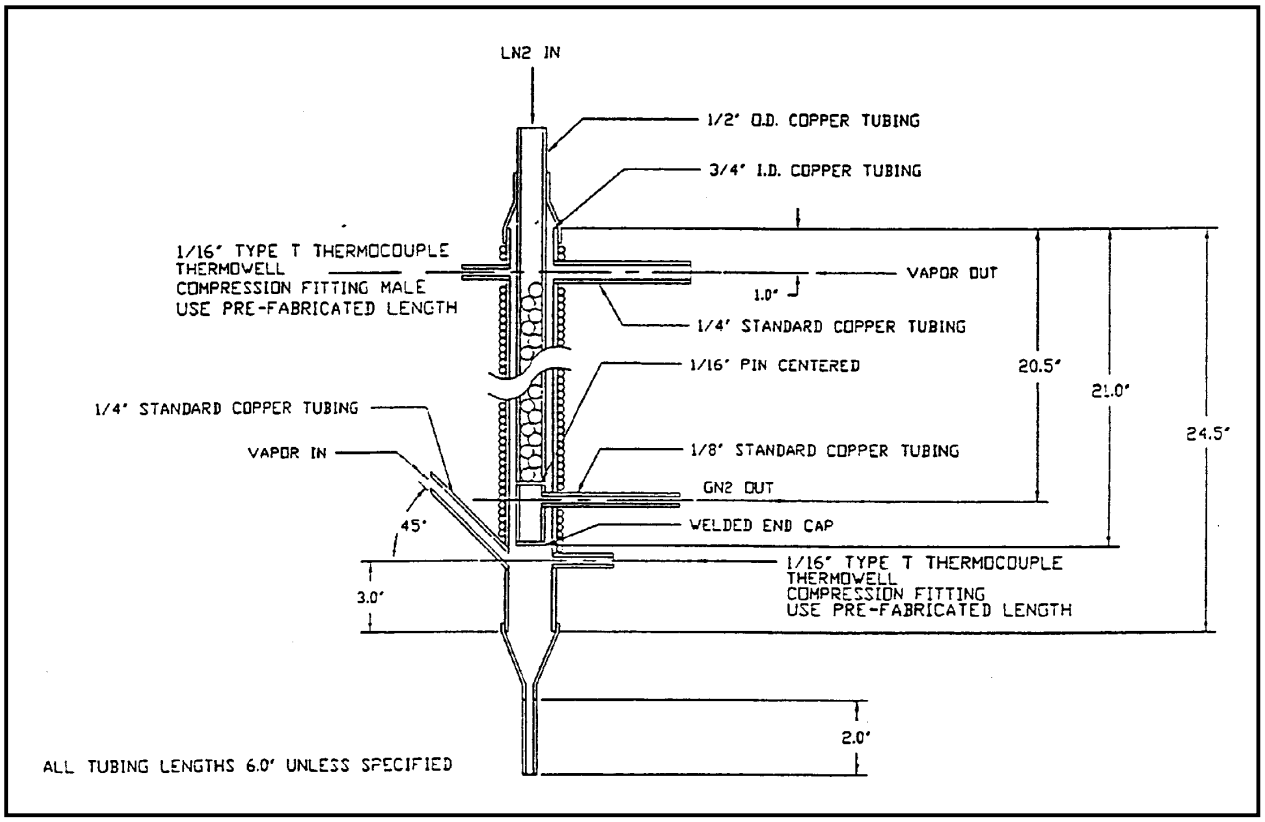

Figure 5. Cross-sectional view of cryogenic condenser.

LN_2 is delivered to the condenser with a self-pressurizing dewar (CryofabTM Model CFPB25-115). Dewars are special vessels, often involving vacuum insulation, designed for storage and handling of cryogenic liquids such as LN_2. The set-point pressure in the dewar is maintained by controlling the amount of LN_2 that passes through a heat exchanger inside the vessel with a cryogenic valve. The LN_2 vaporizes and returns to the LN_2 storage area. The amount of vaporized LN_2 controls the pressure inside the vessel.

The liquid flow rate of LN_2 controls the temperature of the condenser. Flow rate of LN_2, in turn, is controlled by the pressure of the dewar and by a normally closed cryogenic solenoid valve (Asco Red-Hat Series 8264). The cryogenic solenoid valve is controlled using a Gordinier Electronics (Model 259) LN_2 temperature controller. A type T thermocouple mounted inside the shell of the condenser entrance provides the temperature feedback for the temperature controller. If the temperature of the condenser at the thermocouple location is above the setpoint temperature, the controller opens the solenoid valve for LN_2 delivery.

The laboratory-scale condenser was fabricated at the University of Illinois at Urbana-Champaign. The condenser has a surface area of 1241 cm^2. The condenser is made of 99.9 percent pure copper, which was selected for its high thermal conductivity. A 3.8 cm layer of polymeric foam insulation covers the outside of the condenser with an aluminum and vinyl foam insulation around the polymeric insulation as a radiative heat shield. Inlet and outlet tubing is also insulated with polymeric foam insulation wrapped in fiberglass insulation and surrounded by an aluminum radiation shield. The temperature of the TVOC challenge gas stream is monitored using type K thermocouples at the condenser inlet and outlet. The concentration of the TVOC exiting the fixed bed during regeneration and entering the condenser is determined with draw samples injected into the GC/MS.

Analytical Measurement Instruments

Total Hydrocarbon Analyzer/Flame Ionization Detector

Calibration of the gas generation system and monitoring of TVOC concentrations exiting the fixed-bed were performed using a THC analyzer with a FID (Thermo Environmental, Model 51). The instrument contains a calibration routine, which involves sending a given flow rate of "zero" (or clean carrier) gas to the FID, followed by a given flow rate of a gas stream of known concentration. Matheson gas standard cylinder mixtures of 1000 ppmv MEK in N_2 and 1005 ppmv toluene in N_2 were used for these standard gases. As the detector oxidizes the hydrocarbons, ions are generated and the instrument generates an analog voltage output proportional to the TVOC concentration. During calibration, it is important to monitor the pressure of the sample in the FID and to ensure that the analyzer was adjusted for this same pressure for the gas stream during testing of the ACFC adsorption system.

Before performing experiments that involved both humidified air streams and TVOC, the response of the FID to RH was tested. This seemed particularly important given the high solubility of MEK. The FID response was found to decrease by < 4 percent (40 ppmv) between zero and 90 percent RH. To ensure that any MEK losses due to high RH conditions were minimized, the tubing between the fixed-bed exit and the inlet to the FID was insulated.

Gas Chromatograph/Mass Spectrometer

A GC/MS (Hewlett Packard GC 5890 and MS 5971) was used to monitor the concentration variability of the inlet air stream concentration to the fixed bed during adsorption runs. The GC/MS is operated with ChemStation software. General calibration of the instrument was performed using the "Standard Autotune" routine included in the ChemStation program. Experimental methods containing appropriate conditions (e.g., oven temperature, solvent delay, total run time) for analyzing both MEK and toluene were developed and saved through this software as well.

Relative Humidity Sensor

The RH of the humidified air stream was measured using a Vaisala capacitive sensor (Model HMP-233). It was not possible to measure the humidity of the air stream after mixing with the TVOC, because the sensor readings could become unreliable, and the sensor could be damaged. The basic operating principle of the Vaisala instrument is the change in capacitance of a thin polymer film on the sensor. The capacitance varies as this film absorbs water molecules so that deviations in the electrical property can be translated into a change in the relative humidity of the gas stream. Calibration was performed by inter-comparing the sensor with another RH sensor that had been calibrated with deliquescent $(NH_4)_2SO_4$.

Data Acquisition and Control System

The DACS is composed of:

- Keithley 500 series DACS mainframe system (supporting two AIM7 thermocouple cards, one AIM3 high speed 10 mV to 10 V voltage card, one AOM5 +/-1 to 10 V high speed analog output, one AMM2 global amplifier and A/D 16 bits converter module, and an IBIN computer interface card)
- PC computer (Gateway 586-100 MHz)
- Omega OM9-31382AHDI voltage transducer
- Omega OM9-31382AHDI current transducer
- Omega CTL-050005 50:5 current transformer
- Robicon series 440 silicon controller rectifier (SCR)

- STACO Energy variable AC voltage transformer (Variac)
- ViewDAC data acquisition software package (Figure 6).

The DACS automatically measured/controlled and recorded: (1) the temperatures sampling along the fixed bed, (2) applied voltage and current to the fixed bed during the electrothermal regeneration, (3) hydrocarbon concentration with the voltage analog output from the THC/FID, and (4) the applied voltage input to the SCR.

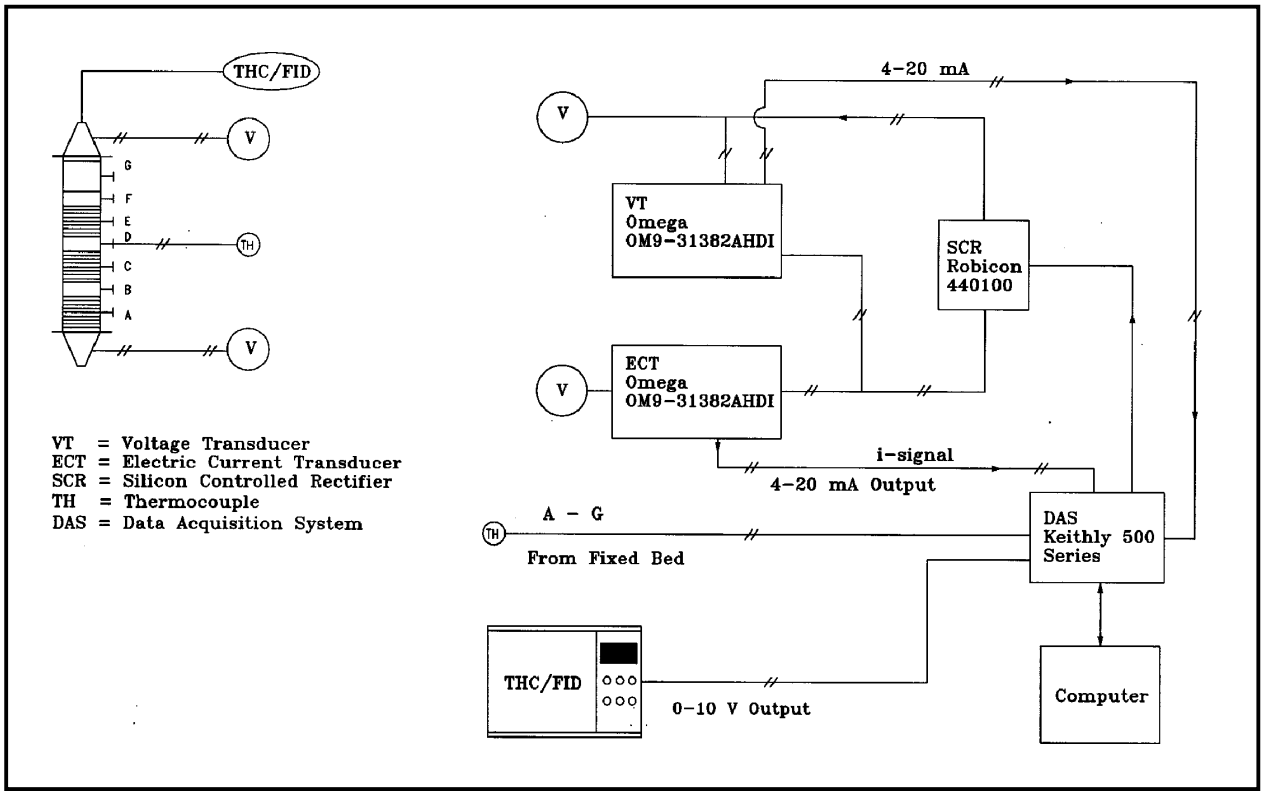

Figure 6. Data acquisition system.

3 Experimental Results and Discussion

Experimental Procedure

The procedure for an adsorption run began with verifying that the fixed-bed had been sufficiently desorbed from the previous experiment. Using a previously-determined adsorption capacity for MEK (Cal et al. 1997), data during the first desorption experiment, and the assumption that the concentration of VOC exiting the fixed-bed during regeneration decreases exponentially, a desorption "standard" was determined. Calculations based on a mass balance indicated that the bed would be more than 99 percent regenerated when the FID reading diminished to 100 ppmv at the elevated temperature associated with 3.0 amps of current and a flow rate of 750 sccm of UHP N_2 through the system. This was used as the desorption "standard" for next adsorption test. The reproducibility of results seen in replicate experiments for all four sets of experimental conditions further validated this standard as adequate. Once the bed was regenerated, the ACFC fixed-bed was cooled and purged with a low flow of UHP N_2.

After cooling the bed to room temperature (23 °C), the FID was calibrated. The air stream containing 1000 ppmv TVOC was then generated, but sent to the exhaust hood rather than through the fixed-bed adsorber, until steady-state conditions existed for TVOC concentration at the outlet of the gas generation system. When the TVOC concentration reached a constant value, draw samples were taken from the gas stream and injected into the GC/MS to provide an average MS peak area associated with the inlet gas stream sent to the hood. At the start of an adsorption test, the TVOC laden air stream was directed through the adsorber. A stopwatch and the DACS system were initiated. The concentration of TVOC exiting the bed was plotted over time in the form of a breakthrough curve on the PC's monitor, and stored on disk with Viewdac software to facilitate monitoring of the experiment. In addition, draw samples were taken upstream of the bed and injected into the GC/MS at approximately 45-minute intervals to verify the consistency of the experimental conditions. At the end of an adsorption run, when the TVOC concentration exiting the fixed-bed remained constant for at least 10 minutes, the TVOC concentration was measured upstream of the adsorber with the THC to verify the absorber's inlet TVOC concentration.

The adsorption experiments resulted in TVOC concentration data as a function of time, to be presented in the form of a breakthrough curve. In addition, this data can be used to determine other important properties of the fixed-bed ACFC system. Of particular interest are the total mass of TVOC adsorbed, the adsorption capacity of the fixed-bed, the length of unused bed (LUB), and the bed throughput ratio (TPR).

The total adsorbed mass of TVOC (M_{sat})(g) can be determined by:

$$\left(M_{sat}\right) = \frac{P\,(MW)\,Q_{air}}{R\,T}\int_{0}^{t_{sat}}\left(\frac{C_{in}}{1-C_{in}} - \frac{C_{out}}{1-C_{out}}\right)dt \qquad \textbf{Eq 1}$$

where:

P = the total pressure (atm)

MW = the molecular weight of the TVOC (g/g-mole)

Q_{air} = the carrier gas flow rate (slpm)

R = the ideal gas constant (atm-l/g-mole-K)

T = the absolute temperature (K)

C_{in} = the concentration of TVOC in the gas stream entering the fixed bed

C_{out} = the concentration of TVOC in the gas stream exiting the fixed bed

t_{sat} = the time at which C_{out} has reached its final, steady-state value and the bed is assumed to be saturated with respect to TVOC (minutes).

The integral term is the area above a breakthrough curve, and has the unit of time.

The adsorption capacity of the fixed-bed is the ratio of the mass of TVOC adsorbed to the mass of ACFC in the bed:

$$\text{Adsorption Capacity} = \frac{M_{sat}}{M_{ACFC}} \qquad \textbf{Eq 2}$$

where M_{ACFC} (g/g) is the mass of ACFC that was used during a saturation experiment.

The adsorption capacity is usually given in units of mg of adsorbate/g of adsorbent. The total mass of ACFC in the fixed bed for all but one of these experiments was 19.2 g. The bed contained 14.6 g of ACFC for the final adsorption experiment, for reasons to be explained later.

The throughput ratio (TPR) for the system is defined as the ratio of the actual volume of gas sent through the system until breakthrough occurred to the ideal or theoretical volume required to completely saturate the adsorption bed:

$$TPR = \left(\frac{t_{5\%}}{t_{50\%}} \right)(100) \qquad \text{Eq 3}$$

TPR describes the ratio of time required for the adsorption bed's outlet TVOC concentration to become 5 percent of its inlet concentration ($t_{5\%}$) to the system's stoichiometric time ($t_{50\%}$). This ratio is typically multiplied by 100 to present the results as percentages. The stoichiometric time is that value associated with 50 percent breakthrough.

A final parameter of importance in evaluating the performance of the adsorption system is the length of unused bed (LUB). LUB describes the percent length of adsorption bed that is not used due to the length of the adsorption zone within the bed:

$$LUB = \left(1 - \frac{M_{5\%}}{M_{sat}} \right)(100) \qquad \text{Eq 4}$$

where:

$M_{5\%}$ = the mass of TVOC adsorbed at 5 percent breakthrough (g/g)

M_{sat} = the mass of TVOC adsorbed when the adsorbent is completely saturated at the adsorption bed's inlet TVOC concentration (g/g).

On saturation of the adsorption bed, UHP N_2 was passed through the ACFC bed and electrothermal desorption was used to regenerate the adsorbent. Electrical power was applied to the adsorber using the electrothermal desorption system (Figure 4) and the DACS (Figure 6). Concentration of TVOC exhausted from the adsorber during desorption, temperature detected within the adsorber at three locations, electrical current consumed, and voltage applied to the ACFC were monitored by the DACS and the results were stored on disk for interpretation.

After completion of each breakthrough test, the saturated ACFC fixed-bed was electrothermally regenerated. In a full-scale system, the fixed-bed can be

conveniently made of several separate modules placed in series. This enables regeneration of each module in a fully saturated condition. Regeneration of a saturated bed enables improved thermal efficiency as well as control of the TVOCs concentration level during desorption.

Regeneration tests for saturated fixed beds of ACFC were performed to evaluate: (1) the effect of applied electrical power on the generated concentration profile, and (2) the difference between the mass of vapor recovered during the desorption to the mass of vapor removed during the adsorption. For all desorption tests, N_2 gas flow rate through the bed was controlled at 1 slpm. The generated desorption stream was diluted with a pure N_2 stream to prevent the concentrated effluent from condensing downstream of the bed and to reduce the concentration to values lower than the upper limit of the THC/FID. The concentration levels of diluted mixtures were measured with the THC/FID by the same procedure as discussed before. The adsorber effluent concentration can be determined using the conservation of mass from the concentration of diluted stream using the following relation:

$$C_c = \frac{C_d\, Q_{N2,t}}{C_d\, Q_{N2,d} + Q_{N2,c}} \qquad \textbf{Eq 5}$$

where:

C_c = concentration of the concentrated TVOC

C_d = diluted TVOC concentration

$Q_{N_2,t}$ = $Q_{N_2,d} + Q_{N_2,c}$ = total nitrogen in the diluted stream (slpm)

$Q_{N_2,d}$ = flow rate of dilution nitrogen added to effluent (slpm)

$Q_{N_2,c}$ = flow rate of nitrogen carrier gas in the fixed-bed (slpm).

Mass of desorbed MEK and toluene was calculated by numerical integration of the concentration profiles in the form of:

$$\left(M_{des}\right)_t = \frac{P\,(MW)\,Q_{N_2}}{R_u\,T} \int_0^t \frac{C_{out}}{1 - C_{out}}\,dt \qquad \textbf{Eq 6}$$

Applied energy was calculated by integration of the power from experimental data:

$$E_t = \int_0^t v.i\,dt \qquad \textbf{Eq 7}$$

where:

v = rms voltage (volts)

i = rms current (amps)

E_t = energy applied until time t

t = time (seconds).

The cryogenic condensation unit was also evaluated during regeneration, as part of the integrated adsorption-regeneration-condensation system for TVOC vapor removal, capture, and recovery. As an adsorption run was approaching saturation, LN_2 was sent through the condenser system, so that the recovery unit would be at its desired setpoint temperature (≈ -40 °C) when the fixed-bed was ready for regeneration. When the adsorption experiment was completed, tubing was adjusted to direct the gas stream exiting the fixed-bed to the condenser. The gas stream exiting the condenser was sent to the FID. During the operation of the cryogenic unit, temperatures at upstream and downstream locations on the condenser were recorded at regular intervals. The TVOC concentration of the gas stream entering the condenser was determined by injecting draw samples to the GC/MS. TVOC concentrations in the gas stream exiting the condenser were read from the FID. In addition, the liquid TVOC recovered from the condenser was later injected to the GC/MS and compared to injected samples of pure liquid TVOC taken from the original bottle for purity analysis.

Adsorption Experimental Results

Experimental results from the adsorption tests of this project are presented in the following sub-section. Triplicate breakthrough curves are provided for each set of experimental conditions in Figures 7, 9, 11, and 13. In addition, Figures 8, 10, 12, and 14 combine the data from the triplicate runs in nondimensionalized form. Normalization of the data provides a good way to compare the reproducibility of replicate adsorption runs performed at similar experimental conditions.

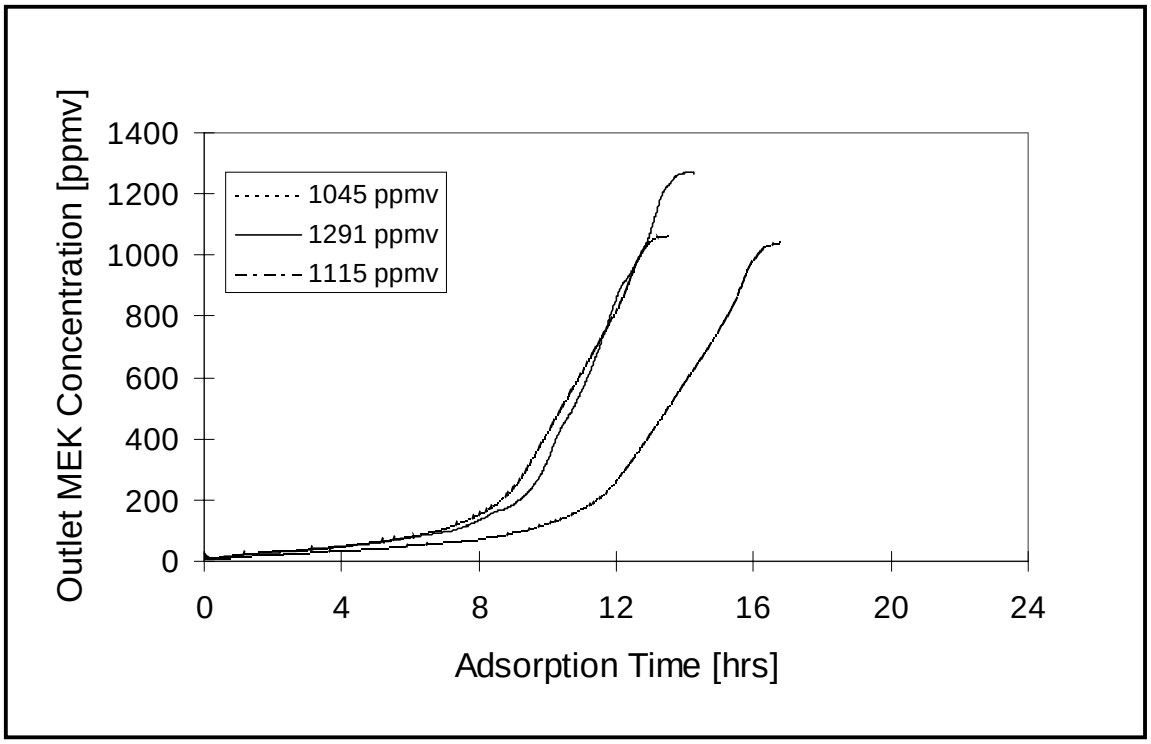

Figure 7. Adsorption breakthrough results for MEK in dry air.

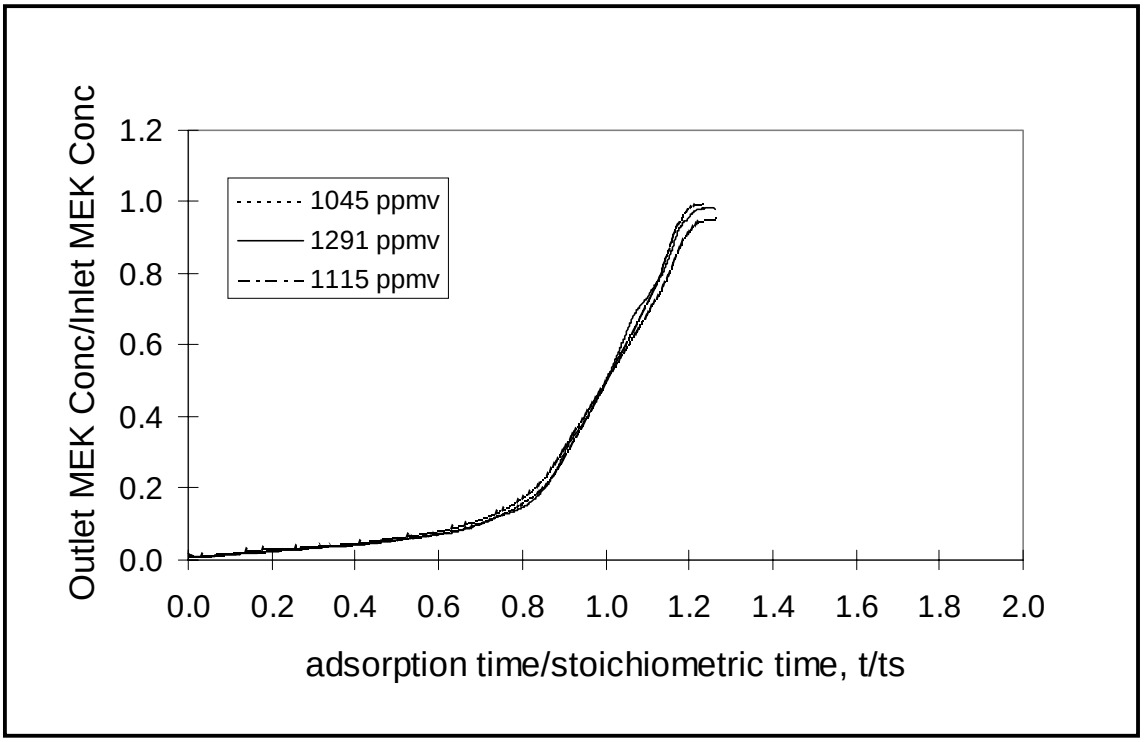

Figure 8. Normalized breakthrough results for MEK in dry air.

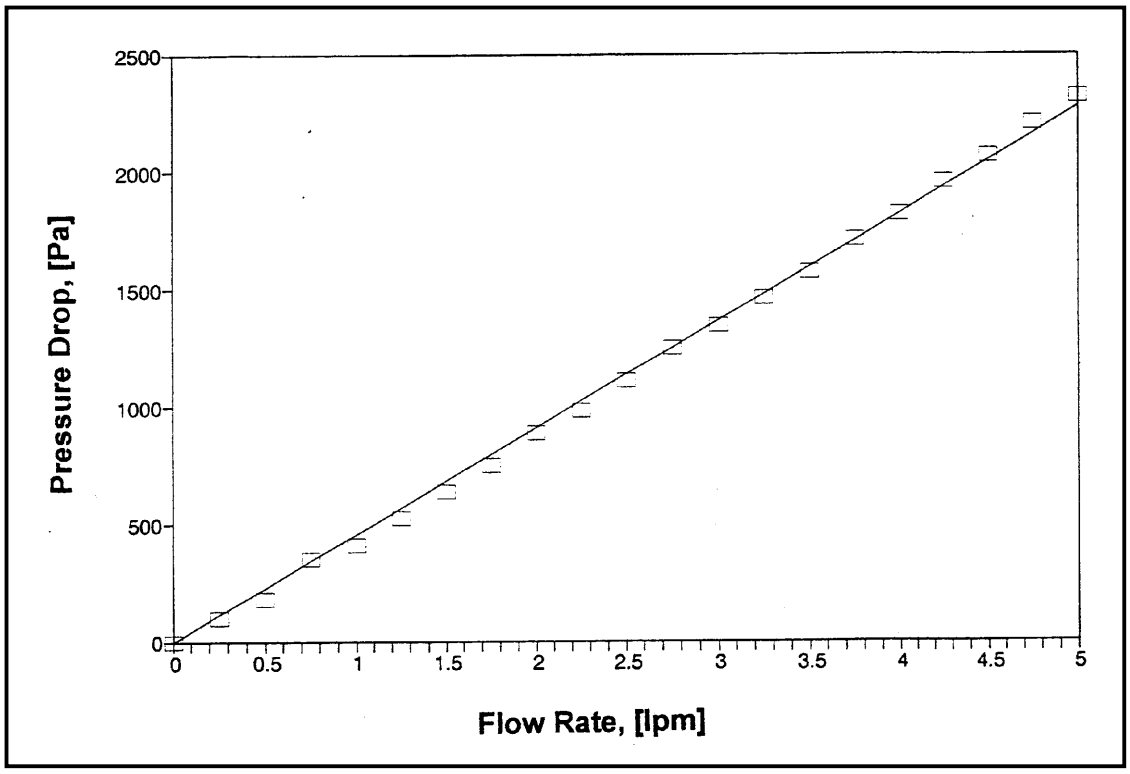

Figure 9. Pressure drop through the ACFC fixed-bed vs. flow rate.

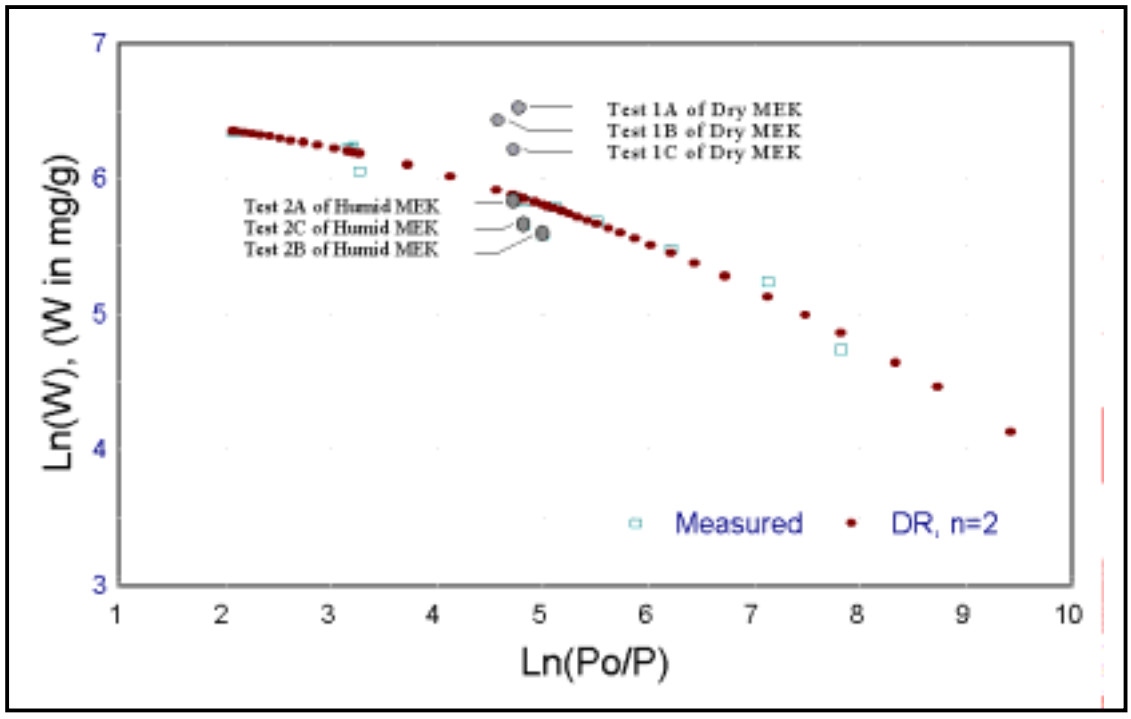

Figure 10. Comparison of present adsorption capacity results to equilibrium data.

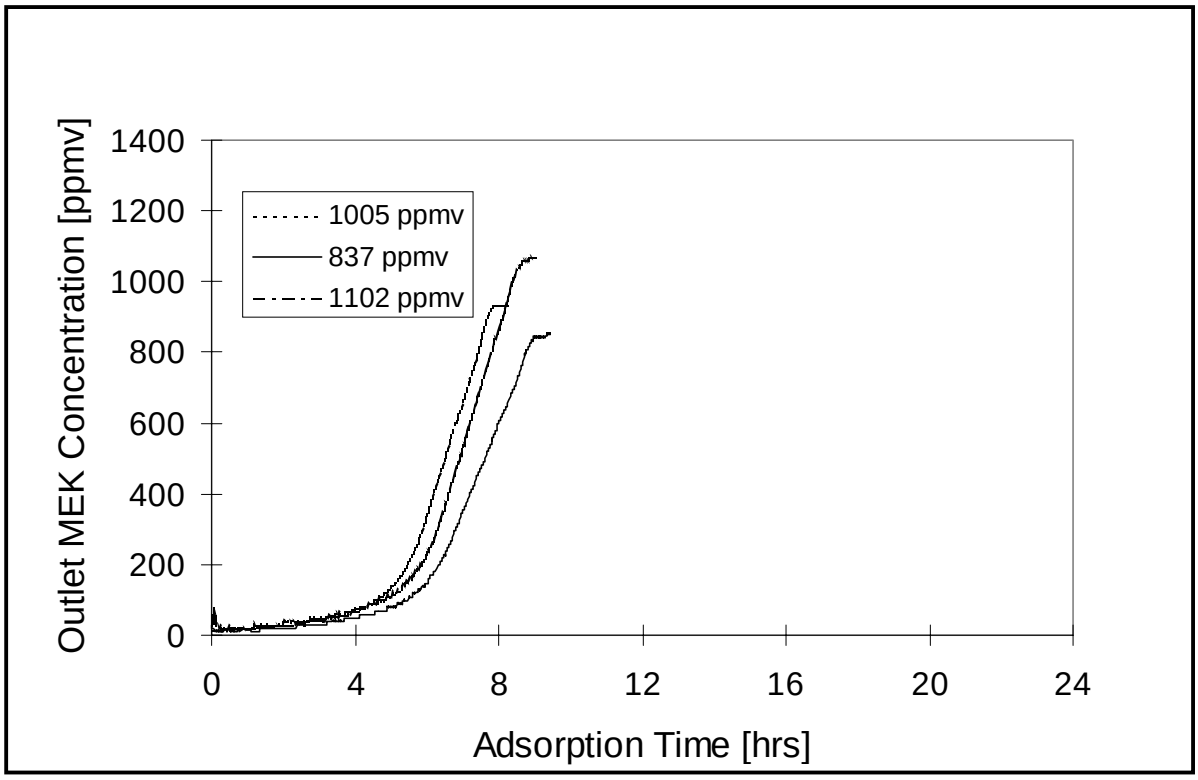

Figure 11. Adsorption breakthrough results for MEK in humid air.

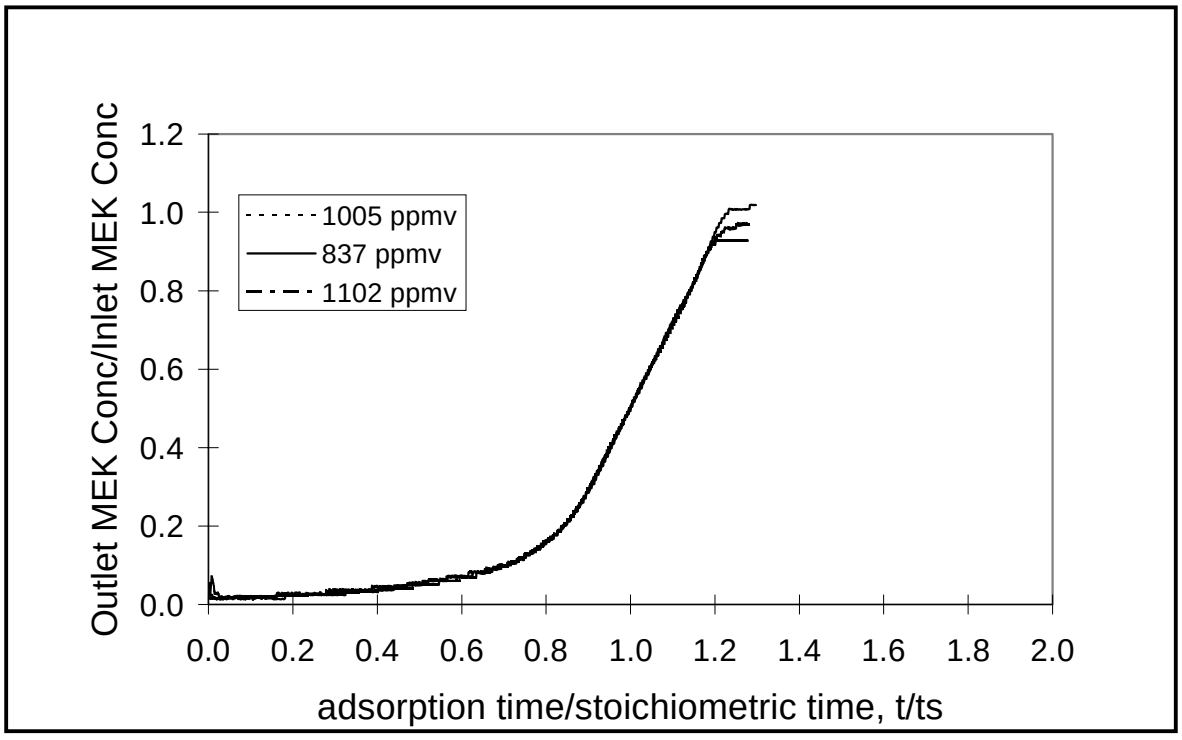

Figure 12. Normalized breakthrough results for MEK in humid air.

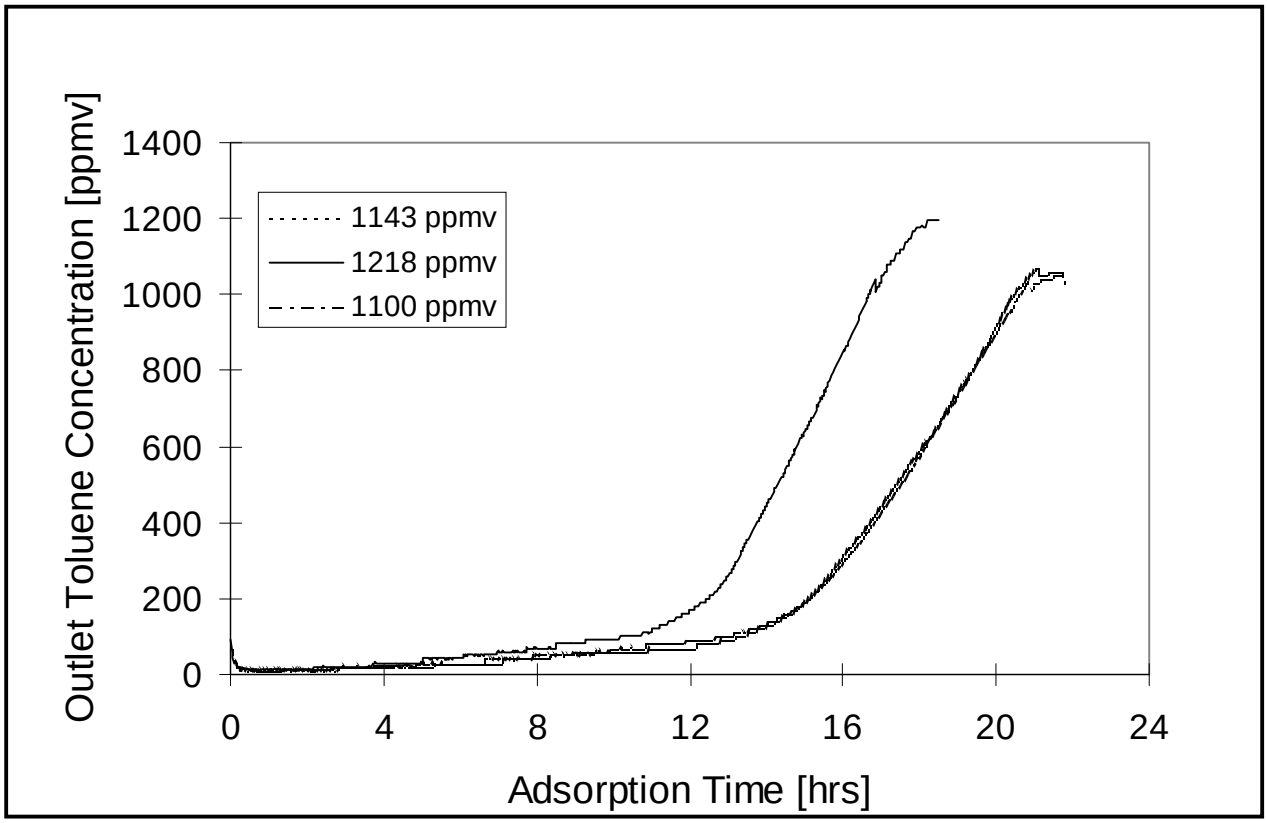

Figure 13. Adsorption breakthrough results for toluene in dry air.

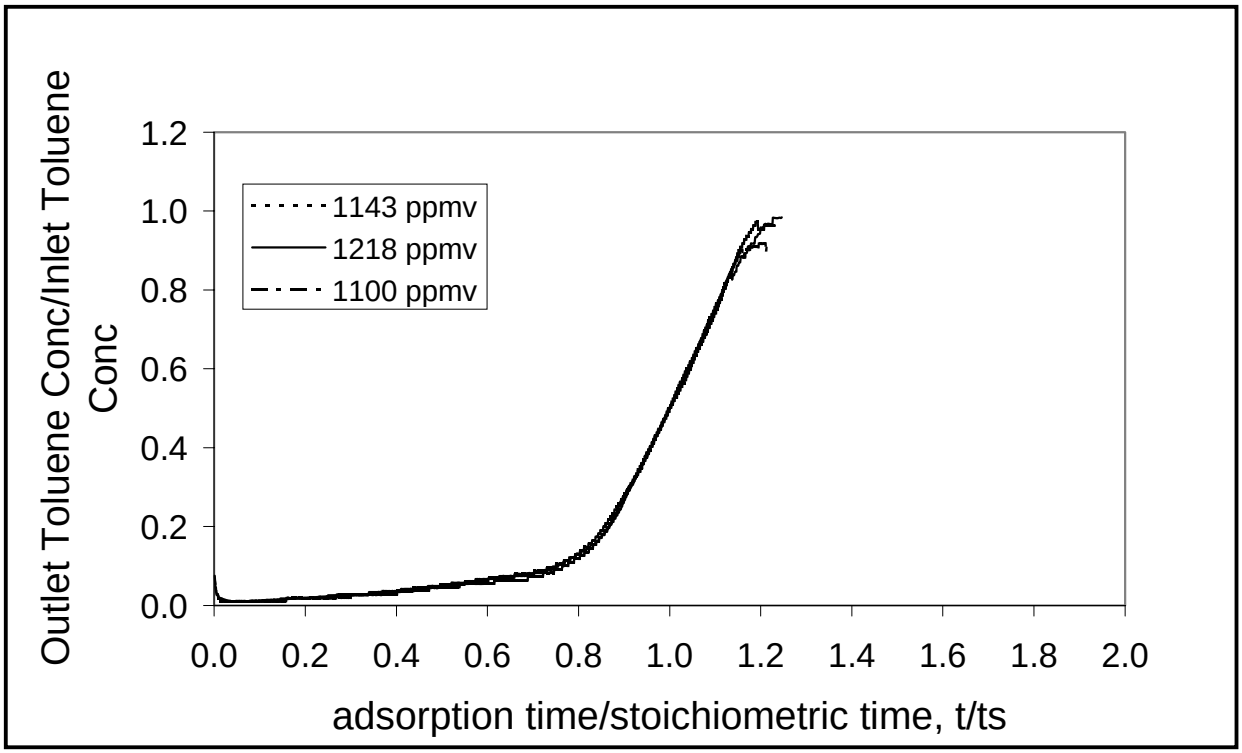

Figure 14. Normalized breakthrough results for toluene in dry air.

In these nondimensionalized plots, the ordinate is given by the ratio of the TVOC concentration exiting the fixed-bed to the inlet TVOC concentration. The abscissa in these figures is given by the ratio of $t/t_{50\%}$, where $t_{50\%}$ is the previously-defined 50 percent breakthrough time of the bed. Given this definition for $t_{50\%}$, all nondimensionalized results should pass through the point ($t/t_{50\%}$ = 1, C(out)/C(in) = 0.5).

Tables 3, 4, 5, and 6 summarize the experimental conditions (total gas flow rate, mean C_{in} and its standard deviation, mean RH_{in} and its standard deviation) during each adsorption test. Also provided in the tables are the adsorption bed performance parameters ($t_{5\%}$, $t_{so\%}$, mass of ACFC, mass of TVOC adsorbed, adsorption capacity, LUB, and TPR) as determined using the experimental data and the equations provided above. Experiments performed under the same set of experimental conditions are represented by the same number (i.e., 1,2,3, and 4); replicates within a set of conditions are differentiated alphabetically (i.e., A,B,C).

Table 3. Parameters for adsorption tests with MEK in dry air.

	1A	1B	1C	Mean	Std. Dev.
Air flow rate, (slpm)	5.4	4.9	4.3	5.1	0.3
Inlet gas concentration, (ppmv)	1045	1291±41	1115±12	1116.7	7.25
Mass of ACFC, (g)	19.2	19.2	19.2	19.2	0
Breakthrough time, $t_{5\%}$ (hrs)	6.1	5.3	4.5	5.3	0.8
Stoichiometric time $t_{50\%}$ (hrs)	13.6	11.3	10.7	11.9	1.5
Mass of MEK adsorbed, (g)	13.0	12.0	9.7	11.6	1.7
Adsorption capacity, (mg/g)	676.6	627.2	503.9	602.6	88.9
LUB, (%)	54.3	52.1	57.4	54.6	2.7
TPR, (%)	44.7	47.0	41.2	44.3	2.9

Table 4. Experimental conditions and parameters for adsorption tests with MEK in humid air.

	2A	2B	2C	Mean	Std. Dev.
Air flow rate, (slpm)	5.0	5.0	5.0	5.0	0.0
Inlet gas concentration, (ppmv)	1005±49	837±61	1102±37	981.3	134.1
Mass of ACFC, (g)	19.2	19.2	19.2	19.2	0.0
Relative humidity	90.1±4.6	91.5±2.7	91.2±2.2	90.9	0.7
Breakthrough time, $t_{5\%}$ (hrs)	3.1	3.7	3.3	3.4	0.3
Stoichiometric time $t_{50\%}$ (hrs)	6.5	7.3	7.1	6.9	0.4
Mass of MEK adsorbed, (g)	5.5	5.2	6.6	5.8	0.7
Adsorption capacity, (mg/g)	288.6	268.1	343.3	300.0	38.9
LUB, (%)	51.1	48.6	52.3	50.7	1.9
TPR, (%)	48.3	50.5	47.0	48.6	1.8

Table 5. Experimental conditions and parameters for adsorption tests with toluene in dry air.

	3A	3B	3C	Mean	Std. Dev.
Air flow rate, (slpm)	5.1	5.1	5.1	5.1	0.0
Inlet gas concentration, (ppmv)	1143±23	1218±46	1100±16	1153.7	59.7
Mass of ACFC, (g)	19.2	19.2	19.2	19.2	0.0
Breakthrough time, $t_{5\%}$ (hrs)	8.9	7.7	8.4	8.3	0.6
Stoichiometric time $t_{50\%}$ (hrs)	18.0	14.8	17.7	16.8	1.7
Mass of toluene adsorbed, (g)	22.6	19.9	21.4	21.3	1.4
Adsorption capacity, (mg/g)	1178.5	1038.0	1113.8	1110.1	70.3
LUB, (%)	49.6	47.3	52.2	49.7	2.4
TPR, (%)	49.5	52.0	47.2	49.6	2.4

Table 6. Experimental conditions and parameters for adsorption tests with toluene in humid air.

	4A	4B	4C	Mean*	Std. Dev*.
Air flow rate, (slpm)	5.1	5.1	5.1	5.1	0.0
Inlet gas concentration, (ppmv)	1053±43	1086±31	1064±50	1067.7	16.8
Mass of ACFC, (g)	19.2	19.2	19.2	19.2	0.0
Relative Humidity	92.5±2.9	91.7±2.2	93.9±3.4	92.7	1.11
Breakthrough time, $t_{5\%}$ (hrs)	5.3	5.8	1.2	5.6	0.3
Stoichiometric time $t_{50\%}$ (hrs)	11.2	11.3	8.9	11.2	0.1
Mass of toluene adsorbed, (g)	13.0	13.8	11.4	13.4	0.6
Adsorption capacity, (mg/g)	675.6	719.7	798.0	697.7	31.2
LUB, (%)	52.0	49.2	88.0	50.6	2.0
TPR, (%)	47.7	51.4	13.4	49.6	2.6
* Mean & Standard Deviation for Tests 4A & 4B Only					

Adsorption of MEK from Dry Air Stream Mixture

The adsorption experiments for dry air containing MEK were the first tests run to evaluate the system's ability to remove TVOCs at inlet concentrations ≈ 1000 ppmv. Generating an air stream that contained 1000 ppmv of MEK proved to be difficult, as was performing all three experiments at the same inlet concentration of the TVOC. This is largely due to the high vapor pressure of MEK (12.6 kPa at 25 °C).

Triplicate adsorption curves for dry MEK in air at ≈ 1000 ppmv are presented in Figure 7. Legends in the figures of the adsorption curves describe the mean inlet concentration of TVOC. The average concentrations leaving the fixed bed over the first 2 hours of Tests 1A, 1B, and 1C were 15.4 ppmv, 18.9 ppmv, and 22.2 ppmv, respectively. Based on the average inlet concentration for each run, these values indicate removal efficiencies of 98.5, 98.5, and 98 percent. Similar removal efficiencies over the first 2 hours of adsorption were observed in other

experiments presented in this report. The overall shapes of these curves indicate similar adsorption dynamics inside the fixed-bed. Discrepancies between the curves are more attributable to differences in the experimental conditions, most notably the total gas flow rate and the inlet TVOC concentration (Table 3). Both of these variables affect the duration of the experiment and the final value of the outlet concentration. The true similarity of these triplicate experiments is demonstrated in Figure 8, where data are presented in nondimensionalized form. The correspondence of the dynamics of adsorption is more obvious, as all three breakthrough curves are nearly identical. Note that, in this figure and all other figures containing nondimensionalized adsorption data, the final normalized concentration may exceed unity. When this occurs, it is because the average inlet concentration over the entire experiment was less than the final, steady-state outlet TVOC concentration.

Table 3 lists the experimental conditions and presents fixed-bed adsorption parameters for the dry MEK tests. Again, mean inlet TVOC concentrations ranged from 1045 to 1291 ppmv, due to the difficulty of repeating the same initial conditions due to the volatility of MEK and adsorption tests exhibiting $t_{50\%}$ values between 10.7 and 13.6 hours. The total volumetric flow rate of air through the system also ranged from 4.8 to 5.4 slpm. Figure 9 shows pressure drop across the fixed-bed as a function of total gas flow rate. Pressure drop demonstrates a linear dependence on total gas flow rate. Correspondence between the calculated parameters in Table 3 provides further evidence of the reproducibility of experimental results seen in Figure 8. In particular, the mean and standard deviation for LUB (54.6 and 2.7 percent, respectively) indicate only 4.9 percent variability in this characterization of the fixed-bed. The variability of the TPR for the three experiments was also only 6.5 percent. The mean $t_{5\%}$ value is 5.3 hours, which is considerable for experimental tests with a laboratory-scale system. The mass uptake of MEK by the ACFC (9.7 to 13.0 g) yields adsorption capacities from 504 to 677 mg/g, with the lower limit corresponding to experiment 1C and the upper limit to experiment 1A. These adsorption capacities are compared to equilibrium data in Figure 10. The adsorption capacity of MEK under dry conditions in the adsorption bed is larger than values previously obtained using a gravimetric balance. Differences in results could be due to the use of different lots of ACFC. In other words, electrical power was applied across the ACFC to regenerate the adsorbent in the bed while elevated gas temperatures were used to regenerate the ACFC used with the gravimetrically determined adsorption tests. Previous desorption tests using electrothermal desorption on a single sheet of ACFC demonstrated < 5 percent change in specific surface area of the ACFC after 50 adsorption-desorption

cycles. The difference in the adsorption capacities needs to be further evaluated in follow-up studies.

Adsorption of MEK From Humid Air Stream Mixture

Figure 11 shows the breakthrough curves during triplicate adsorption experiments in which the ACFC was exposed to a challenge gas stream at ≈ 90 percent RH and containing ≈ 1000 ppmv of MEK. As for the tests with MEK in a dry air stream, the breakthrough curves are all similar in their general form although variations in the exact inlet TVOC concentration result in different final TVOC outlet concentrations and different experimental run times. Figure 12 (which gives the breakthrough data in nondimensionalized form) again shows the true similarity of adsorption dynamics in the bed for this multi-component inlet gas stream.

Table 4 summarizes the experimental conditions for tests 2A to 2C. For these experiments, the total gas flow rate was kept constant across all three runs, as compared to 6.5 percent variation for the dry MEK tests, though some variability still exists in the inlet MEK concentration due to the TVOC's vapor pressure. This table highlights the performance of the automated humidifier system, as evidenced by the maintenance of RHs with very little deviation from the 90 percent RH setpoint, during experiments lasting nearly 9 hours. Many of the adsorption parameters calculated with the experimental data also show a high degree of correspondence for this set of runs. The mass of MEK adsorbed during the full saturation experiment ranged from 5.2 g (test 2B) to 6.6 g (test 2C), with corresponding adsorption capacities between 268 mg/g and 343 mg/g. These results are again compared to equilibrium adsorption capacities in Figure 10.

Results from these tests must also be compared to those presented for the MEK adsorption tests performed in a dry air stream, to examine the effect of the water vapor on the ACFC fixed-bed system. Although LUB for the humidified tests are only 4 percent less than for the dry test conditions, $t_{5\%}$ values, total mass of MEK adsorbed, and adsorption capacities are all reduced by a greater percentage for the experiments at elevated RH conditions. The mean $t_{5\%}$ value for humid conditions is 64 percent of the corresponding value for dry tests. In addition, the mass of MEK adsorbed (and thus the adsorption capacity) has been reduced by 50 percent. This is evidence that competitive adsorption occurs between the water vapor, MEK, and ACFC, with water vapor occupying sites that had adsorbed MEK during the experiments performed with dry air. This is an important phenomenon to have observed, since the effect of water vapor on TVOC adsorption is not easily predicted.

Adsorption of Toluene From Dry Air Stream Mixture

The equilibrium vapor pressure of toluene (3.8 kPa at 25 °C) is 70 percent lower than the equilibrium vapor pressure of MEK at 25 °C, which enhanced the ability to perform triplicate adsorption experiments for toluene in dry air at more constant conditions. Figure 13 shows two of the adsorption curves to be nearly identical. The more rapid breakthrough of the curve for test 3B (C_{in} = 1218 ppmv) is due to the higher inlet TVOC concentration at which this test was performed. When the experimental results are normalized by each test's average inlet TVOC concentration and $t_{50\%}$ values (Figure 14), all three data sets again exhibit high reproducibility in terms of ACFC adsorption dynamics.

Table 5 lists data that quantify the bed's pollution control performance. Note that the fixed-bed did not reach the $t_{5\%}$ point until 7.7 to 8.9 hours after the beginning of the test. If a 5.3 cm/sec superficial gas velocity is a good estimate for the velocity of the TVOC-laden to be captured by an industrial process, then the resulting $t_{5\%}$ value is a sufficient duration without the need for adsorption system scale-up issues. The calculated values for the total mass of toluene adsorbed, and thus the adsorption capacity of the ACFC for toluene, are also remarkably high for these experiments. The average mass of adsorbed toluene for the three tests was 21.3 g, which is greater than the mass of carbon in the fixed-bed. Such high adsorption capacities have yet to be resolved considering the high degree of reproducibility of the tests. The concentration of the standard cylinder of toluene used for FID calibration in these experiments was verified using the FID and a separate standard cylinder of the same concentration. This eliminates inaccurate calibration standards as a possible explanation for the high adsorption capacity results. These results need to be further analyzed in the second phase of the project. Finally, note that the mean LUB and TPR values for the dry toluene experiments were 49.7 and 49.6 percent, respectively, as compared to 50.7 and 48.6 percent for the humidified MEK tests, and 54.6 and 44.3 percent for the dry MEK tests. This suggests a certain consistency of performance for ACFC when adsorbing toluene or MEK, even if the RH is ≈ 90 percent.

Adsorption of Toluene from Humid Air Stream Mixture

Breakthrough curves for this set of experimental conditions (≈ 1000 ppmv toluene in air at RH ≈ 90 percent), in their original and nondimensionalized form are provided in Figures 15 and 16, respectively**.** Even without close inspection, these figures clearly show that the third adsorption experiment test (C_{in} = 1064 ppmv) yields different results than the first two similar breakthrough tests.

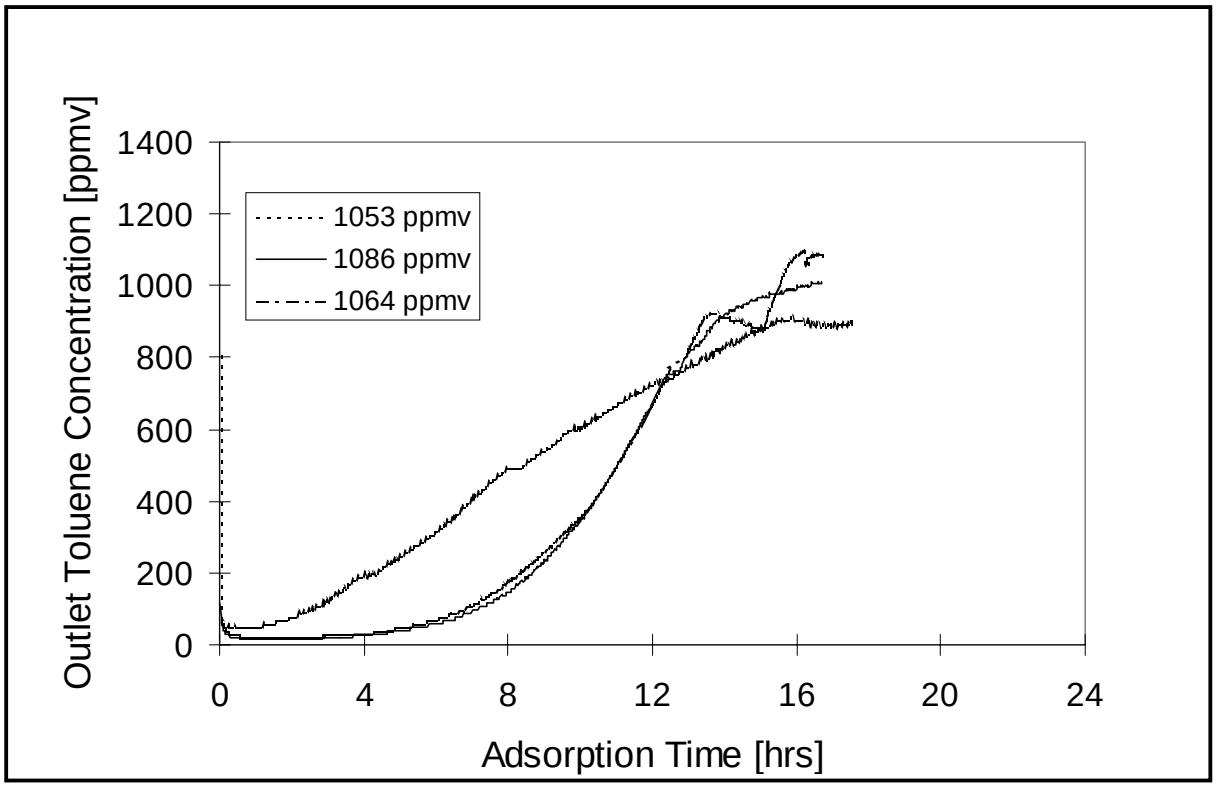

Figure 15. Adsorption breakthrough results for toluene in humid air.

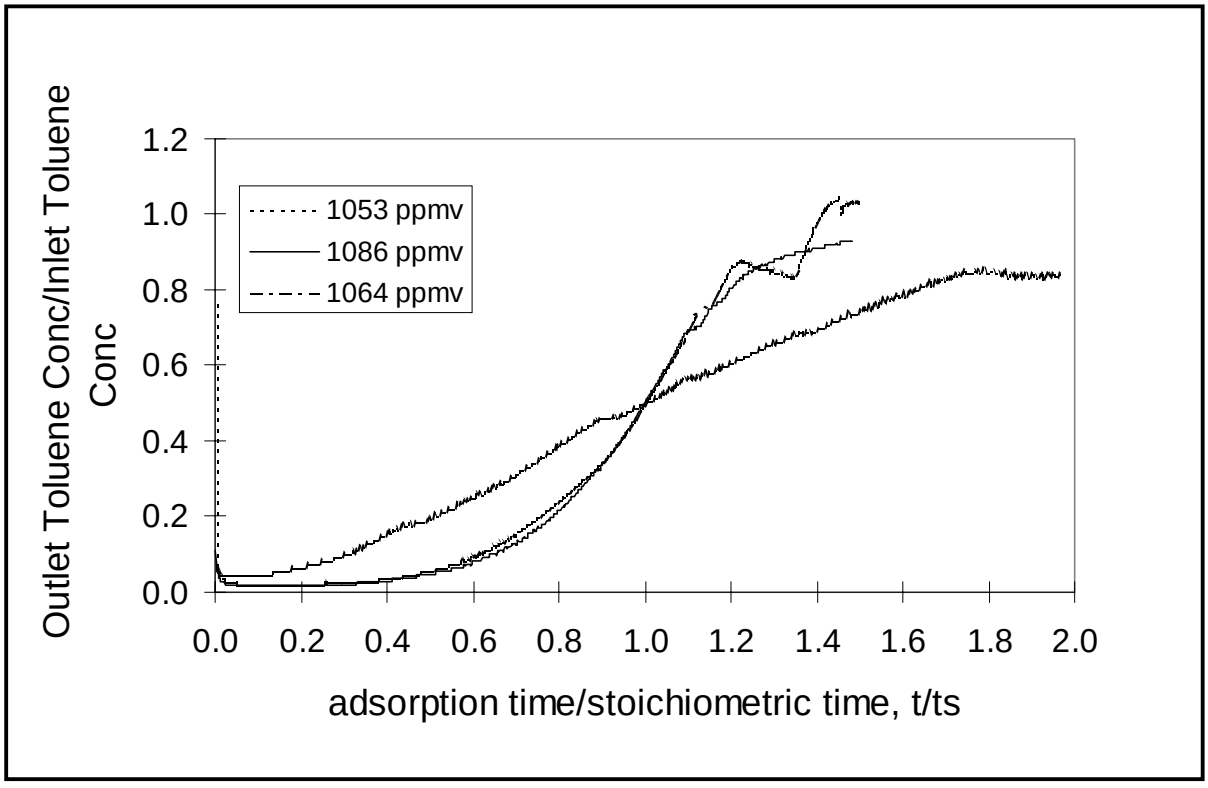

Figure 16. Normalized breakthrough results for toluene in humid air.

The anomalous results from test 4C are due to a change in the fixed-bed configuration for this final experiment. During regeneration of the ACFC following the second experiment for these conditions, a 0.25 cm diameter hole formed in the first module where the electrical regenerator's electrode was located near the ACFC instead of being attached to the stainless steel frame of the pleated ACFC. One possible scenario is that electrical current short circuited through the initial pleat of ACFC instead of through the stainless steel frame for the pleated ACFC. Although N_2 carrier gas was used during the desorption test, the oxygen in the adsorbed water may have contributed to the apparent selective oxidation of the ACFC. The adsorber was dismantled and the adsorbent was replaced. In an effort to see if the adsorption bed could operate at 1000 ppmv TVOC with a shortened bed length and due to the duration of many of the adsorption experiments performed, the final adsorption test was done with two instead of three modules. The fixed-bed was thus rebuilt with two ACFC modules, with a total mass of ACFC of 14.6 g of adsorbent material.

The results from the third breakthrough curve (1064 ppmv, Figures 15 and 16) suggest that this shortening of the fixed-bed length and decrease in adsorbent mass substantially diminished the performance of the adsorption system. The rapid breakthrough of the bed and the overall shape of this adsorption curve indicate that three modules of ACFC are in fact necessary for full development of the adsorption zone inside the fixed-bed for these experimental conditions. The bed must be further characterized with only two ACFC modules during phase two of this project to explain better the results from the third test presented here, and to assess the viability of future fixed-bed designs involving shortened bed length or decreased carbon mass.

The first and second breakthrough tests, in particular the first 12 hours of these adsorption experiments, demonstrate a high degree of reproducibility in adsorption behavior and fixed-bed performance. The brief decrease in outlet concentration during the first adsorption run is not well understood. Post-experimental calculations with the data from these two runs show that the variability in behavior in the first experiment had little effect on the operational parameters used to summarize the adsorption tests (Table 6). Table 6 gives the results of calculations describing breakthrough times and mass-based ACFC adsorption performance from the triplicate tests, and the experimental conditions. For Tests 4A and 4B, the total flow rate of air, the inlet TVOC concentration, and the RH of the TVOC-laden air stream were all within 1.6 percent of each other. Values for $t_{5\%}$ and $t_{50\%}$, total mass of toluene adsorbed, toluene adsorption capacity, LUB and TPR show very little variability when comparing results from Tests 4A and 4B. Breakthrough times at 5 and 50

percent exhibit variabilities of 5.4 and 0.9 percent, respectively. The adsorption capacities for these tests varied 4.5 percent from one another. LUB and TPR varied by 4.0 and 5.2 percent, respectively.

Finally, it is important to compare the calculated results from the toluene adsorption tests performed in dry and in humid air streams. High RH in the inlet gas stream decreased the average 5 percent breakthrough time (discounting the results from the third humidified toluene run) by 33 percent. In addition, the average total mass of toluene adsorbed and adsorption capacity declined by 37 percent. The magnitude of the effect on the 5 percent breakthrough time is thus similar for toluene to what was observed for MEK (30 percent reduction). However, high RH appears to have affected the adsorption capacity of the ACFC for toluene (37 percent) less than was the case for the MEK experiments (a reduction of nearly 50 percent). The reduction in adsorption capacity for toluene is again evidence of competitive effects between water vapor and TVOC for sites on the ACFC. Note once more that TPR and LUB values for humidified toluene-air tests are similar to those determined for all other experimental conditions.

Desorption Experimental Results

Desorption of MEK From Dry Air Stream

Two electrothermal regeneration tests were performed for ACFC fixed beds saturated at the adsorption conditions described in Table 3. Test numbers for the desorption tests correspond to the same numbers for the adsorption tests. Due to the initial development of the automated electrothermal regeneration system, the SCR was not used for the initial experiments. The applied electrical voltage was manually controlled. Electrical voltage for each test was set at select values to observe the effect of applied electrical power. Figure 17 shows the resulting adsorption bed's outlet MEK concentration (top panel, C), normalized MEK mass desorbed (top panel, M), temperature detected inside the ACFC fixed bed for the first MEK desorption test (middle panel, T1, T2 and T3), and electrical power/energy (lowest panel). Maximum MEK concentrations were 9.73 and 10.1 percent by volume. These values are close to the MEK saturation vapor pressure of 12.4 percent. Supersaturated MEK concentrations can be generated applying higher power to the ACFC. Applying higher electrical power to ACFC modules was not tried to prevent generation of local hot spots at the contact points of ACFC layers with the fixed-bed walls. The walls of the existing bed are Teflon®, which can deform at temperatures above 240 °C.

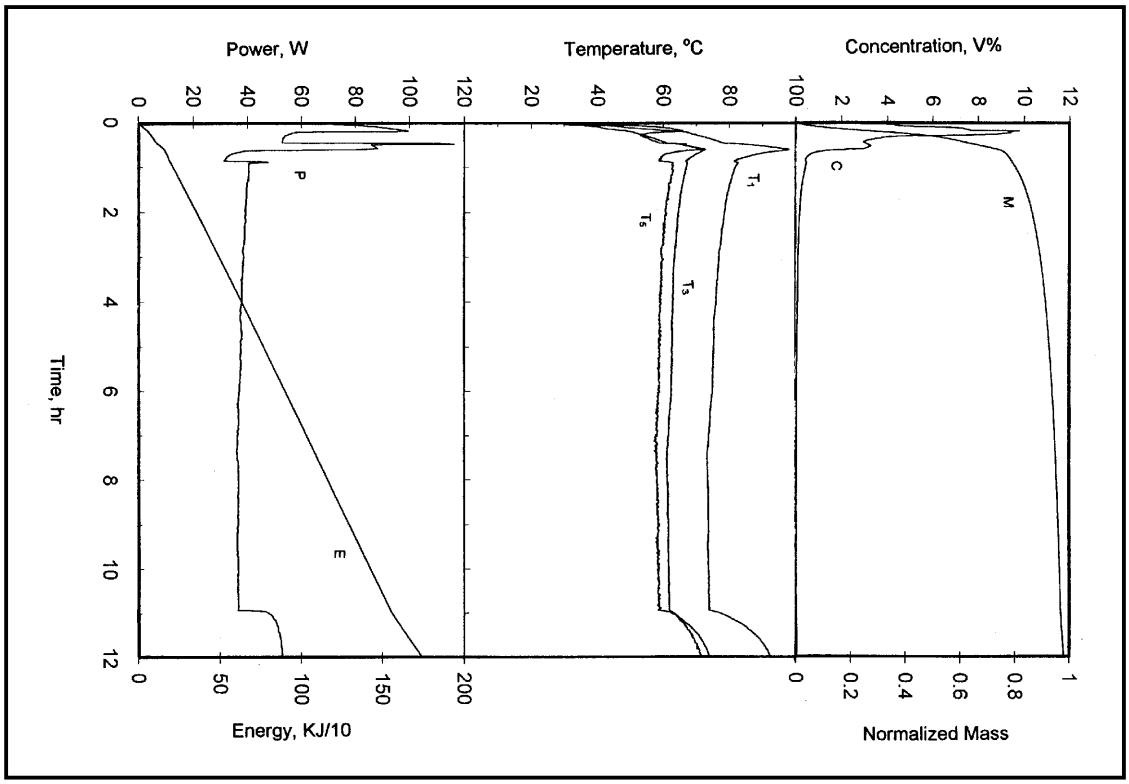

Figure 17. Desorption results for single component MEK.

The measured temperatures were detected between the ACFC modules (Figure 3). Therefore, the ACFC material experienced higher temperatures than the measured values. Temperature in the bed may reach its maximum value close to the bed walls because: (1) the ACFC directly contacts the Teflon® walls, (2) heat convection is minimum on the walls, and (3) Teflon® is a thermal insulator. Alternate control schemes for optimizing the desorption process and alternate adsorber wall composition or configuration of ACFC pleats near the Teflon® walls should be considered during the second phase of the research project.

Under the applied low energy conditions, 80 percent of the bed was regenerated in < 1 hour. Desorption of the remaining 20 percent MEK mass requires an order of magnitude more energy and time. Comparing these results with the results of previous tests for acetone indicates that the initial applied electrical power is very important for increasing the recovery efficiency of MEK (USEPA 1995). Due to the lower boiling point temperature and adsorption energy of acetone, more than 95 percent of the adsorbed mass was regenerated in < 30 minutes by applying high initial electrical power. Table 7 lists the parameters describing these desorption experiments.

Table 7. Regeneration tests for desorption of MEK in dry air.

Test Number	1C	1A
Maximum generated concentration, C_{max}, (%)	9.73	10.1
Time of C_{max}, t_{max}, (min)	12.2	7.47
Mass of MEK regenerated by t_{max}, (g)	2.05	1.57
Energy spent to t_{max}, E_{max}, (KJ)	57	52
Maximum bed temperature at C_{max}, (^{O}C)	66	72
Time of 50% regeneration, (min)	19.1	12.34
Concentration at 50% regeneration $t_{50\%}$, (min)	4.7	6.3
Total MEK mass regenerated (g)	8.11	6.24
Energy spent to $t_{50\%}$, $E_{50\%}$, (KJ)	82.3	78.6
Maximum temperature measured at $t_{50\%}$, (^{O}C)	66	77.2
Carrier gas flow rate, slpm	1	1

These results indicate that more than 50 percent of the adsorbed MEK was regenerated at the effluent temperature of < 50 °C. These low temperatures indicate efficient energy transfer. The calculated mass desorbed is less than the initial amount of adsorption, given in the section describing adsorption of MEK. A hypothesis for the observed mass loss might be due to dissociation of adsorbate on the surface of ACFC when high electrical power is supplied to the bed. The differences in mass of MEK adsorbed to mass of MEK desorbed needs to be further investigated in the second phase of the research project.

Desorption of MEK From Humid Air Stream

Table 8 describes three electrothermal regeneration tests for the ACFC fixed bed saturated with the MEK/H_2O/air gas streams. Table 4 listed conditions during adsorption before these tests with corresponding test numbers. Electrical voltage for each test was set at select values to observe the effect of applied electrical power on the adsorption bed's outlet MEK concentration profile.

Table 8. Regeneration tests for desorption of MEK in humid air.

Test number	2A	2B	2C
Maximum generated concentration, C_{max}, (%)	4.8	7.9	7.4
Time of C_{max}, t_{max}, (min)	32.2	8.57	7.38
Mass of MEK regenerated by t_{max}, (g)	2.23	0.315	0.72
Energy spent to t_{max}, E_{max}, (KJ)	128	71.8	69.4
Maximum bed temperature at C_{max}, (^{O}C)	71	82	89
Time of 50% regeneration, (min)	35.5	34	27.3
Concentration at 50% regeneration $t_{50\%}$, (min)	3.7	3.57	1.31
Total MEK mass regenerated (g)	5.3	4.5	4.254
Energy spent to $t_{50\%}$, $E_{50\%}$, (KJ)	151	192	175
Maximum temperature measured at $t_{50\%}$, (^{O}C)	89	101	104
Carrier gas flow rate, slpm	1	1	1

Figure 18 shows the resulting adsorption bed's outlet MEK concentration (top panel), normalized MEK mass desorbed (top panel), temperature detected inside the ACFC fixed bed for the first MEK desorption test (middle panel, T1, T2 and T3), and electrical power/energy (lowest panel). Maximum MEK concentrations at the outlet of the adsorption bed were 4.8 percent, 7.9, and 7.4 percent by volume. These values are ~50 percent less than those of the previous tests for single component MEK desorption. Results for water vapor are needed to be able to completely analyze the desorption results.

Measurement of water vapor concentration in the carrier gas was left for further investigation due to the complexity of required procedures and resources. During the desorption experiments, condensation of water was observed in the tubing at the outlet of the adsorption bed. This behavior may have caused some of the oscillations that can be seen in the outlet MEK concentration profiles. Increase in the initial electrical power appreciably increases the maximum outlet MEK concentration and shortens the time of regeneration. Compared to single component desorption tests, much more energy is required to produce high MEK concentrations. This can be seen by comparing $E_{max}/E_{50\%}$, $t_{max}/t_{50\%}$, and $C_{max}/C_{50\%}$ values of the MEK/H_2O test results with those of the dry MEK desorption values given in the previous section. Such behavior is caused by an appreciable amount of energy that is transformed to the sensible and latent heat of water vapor during desorption. The mass of MEK regenerated was about half of its initially adsorbed amount in the bed for all three experiments. A comparison of the results of these tests clearly shows that the history of applied power plays a crucial role on the desorption time and profile. Additional experiments will be required for a matrix of systematic experimental conditions during the second phase of the research project to fully characterize the electrothermal desorption,.

Desorption of Toluene From Dry Air Stream

Two experiments were performed for desorption of toluene from the saturated ACFC fixed bed at dry conditions. Initial conditions of the desorption experiments were the same as the saturated end point conditions of the adsorption tests that were described in Table 5. Figure 19 shows the resulting adsorption bed's outlet toluene concentration (top panel), normalized MEK mass desorbed (top panel), temperature detected inside the ACFC fixed bed (middle panel, T1, T2 and T3), and electrical power/energy (lowest panel). Table 9 provides the corresponding summary of the measured and calculated experimental results for both desorption tests.

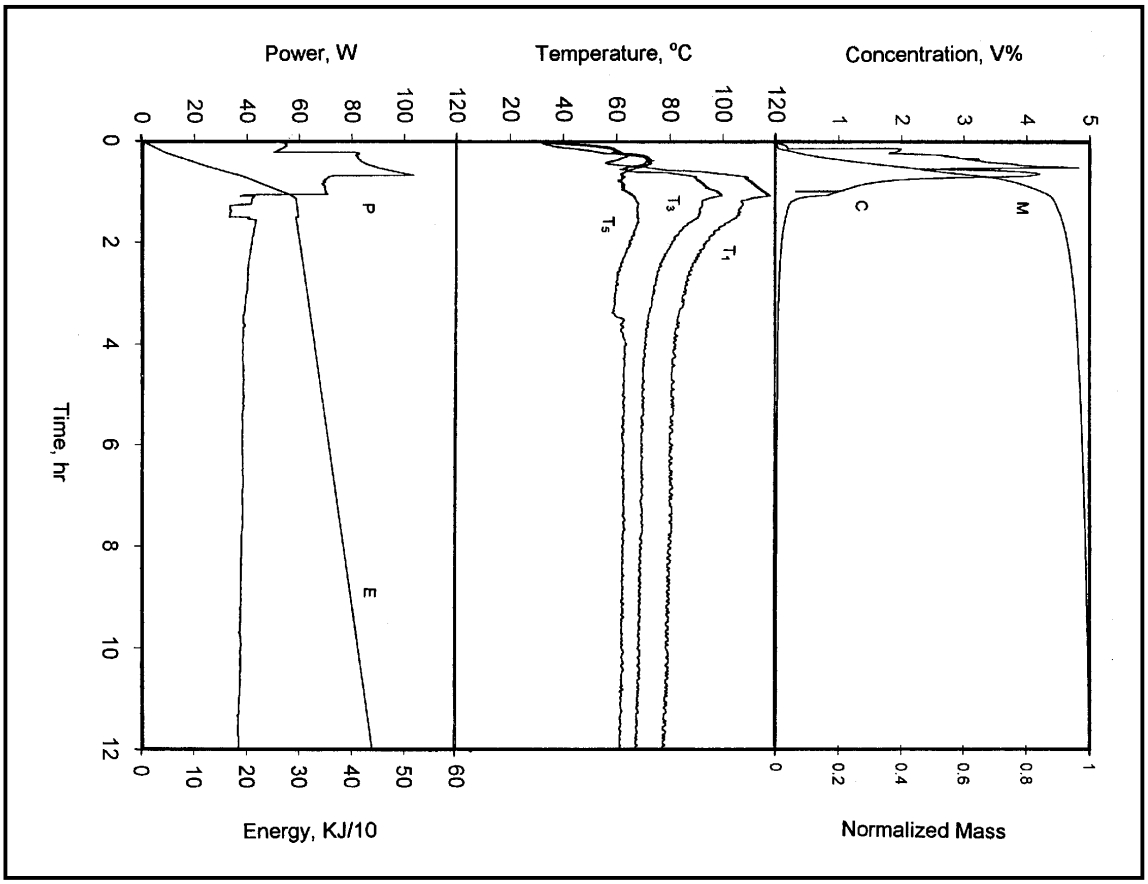

Figure 18. Results for MEK desorption from H_2O/toluene adsorbed condition.

Due to higher toluene molar energy of adsorption, more electrical power is required to produce desorbed toluene concentrations comparable to the ones observed for the MEK desorption experiments. Higher supplied electrical power resulted in lower toluene concentrations of 8.2 and 8.7 percent, by volume. These concentrations are much higher than the saturation vapor pressure of toluene of 3.75 percent by volume. It was observed that the desorption of toluene is much slower than the desorption of MEK and requires more energy. This is due to the higher boiling point temperature of toluene and higher adsorption energy as compared to MEK.

Desorption of Toluene From Humid Air Stream

Two electrothermal regeneration tests were also performed for the ACFC fixed bed that was saturated with toluene/H_2O/air gas streams. Conditions during adsorption before these tests are given in Table 6 with corresponding test numbers. Electrical voltage for each test was set at select values to observe the effect of applied electrical power on the concentration profile.

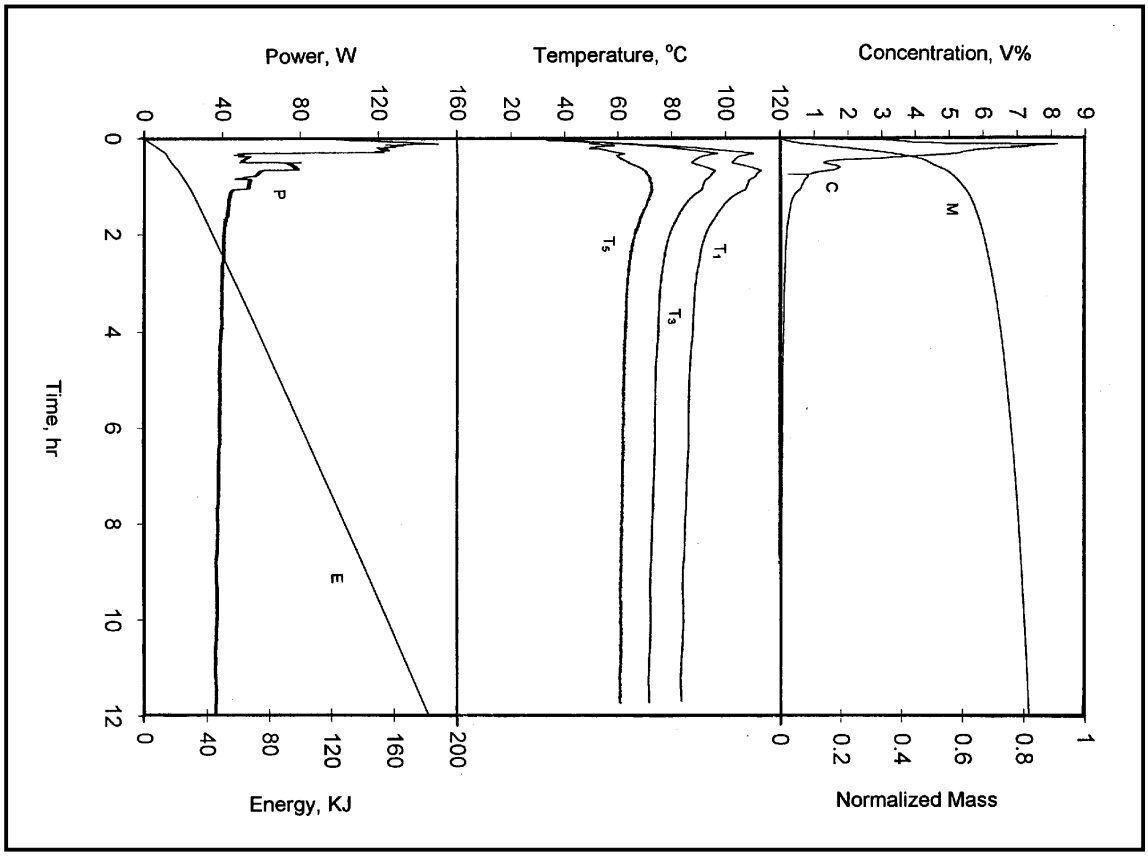

Figure 19. Desorption results for single component toluene.

Table 9. Regeneration tests for desorption of toluene in dry air.

Test numbers	3A	3B
Maximum generated concentration, C_{max}, (%)	8.2	8.7
Time of C_{max}, t_{max}, (min)	8.83	5.13
Mass of toluene regenerated by t_{max}, (g)	1.22	0.81
Energy spent to t_{max}, E_{max}, (KJ)	61.3	53.3
Maximum bed temperature at C_{max}, (^{O}C)	74	75
Time of 50% regeneration, (min)	33.5	19.27
Concentration at 50% regeneration $t_{50\%}$, (min)	1.5	3.49
Total toluene mass regenerated (g)	11.76	9.69
Energy spent to $t_{50\%}$, $E_{50\%}$, (KJ)	184.3	149
Maximum temperature measured at $t_{50\%}$, (^{O}C)	106	107
Carrier gas flow rate, slpm	1	1

Figure 20 shows the resulting adsorption bed's outlet toluene concentration (top panel), normalized toluene mass desorbed (top panel), temperature detected inside the ACFC fixed bed (middle panel, T1, T2 and T3), and electrical power/energy (lowest panel) for the first desorption test. Table 10 summarizes the experimental results. Maximum toluene concentrations were 5.16 and 5.11 percent by volume. These values are less than those of the previous tests for single component toluene desorption, but still higher than those of the tests for toluene saturation vapor pressure. An increase in electrical power does not appreciably increase the generated maximum concentration of desorbed toluene, but appreciably shortens the time of regeneration. Compared to single component desorption tests, much more energy is required to produce high concentrations of toluene. Compared to MEK/H_2O desorption tests, more time is required for the same percentage desorption indicated by the regenerated normalized toluene mass profile. The fact that the boiling point temperature of toluene (110 °C) is higher than that of water is hypothesized to be a major factor for this observation.

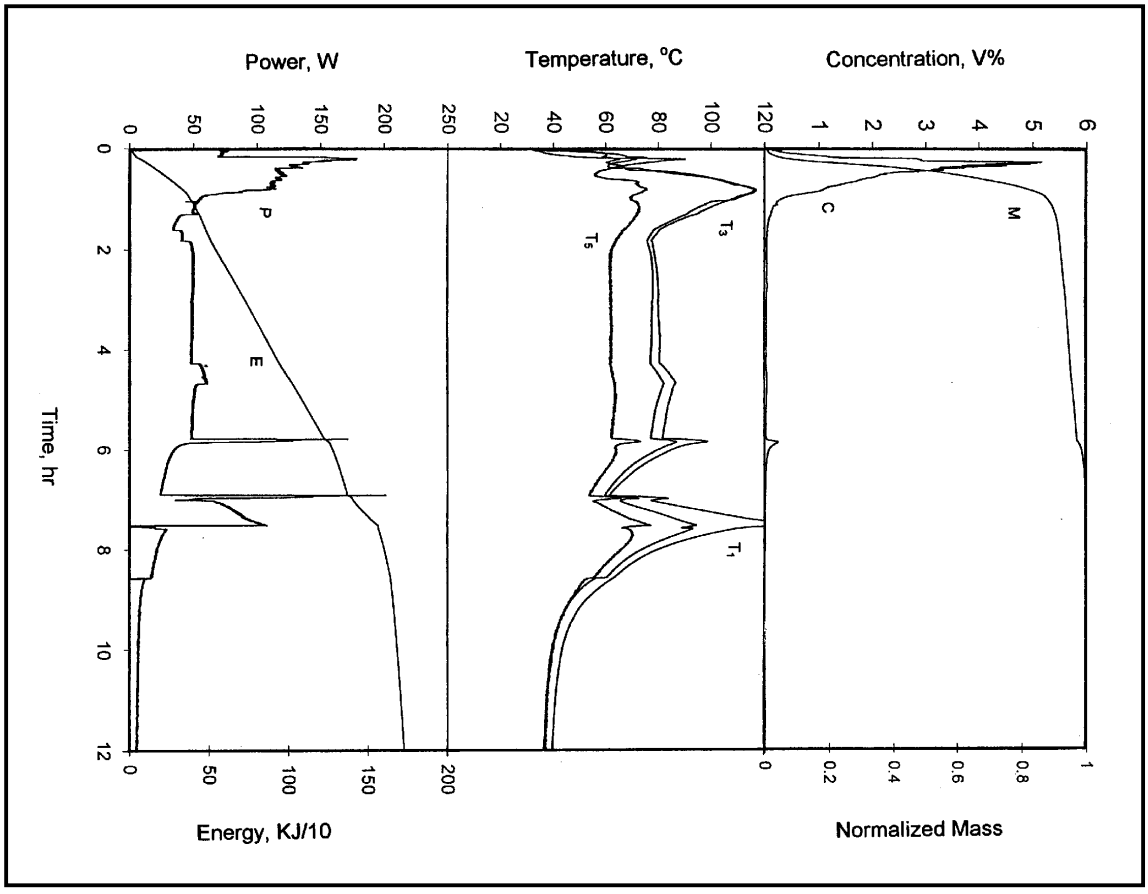

Figure 20. Results for toluene desorption from H_2O/toluene adsorbed condition.

Table 10. Summary of regeneration tests for desorption of toluene in humid air.

Test numbers	4A	4C
Maximum generated concentration, C_{max}, (%)	5.16	5.11
Time of C_{max}, t_{max}, (min)	16.2	5.17
Mass regenerated by t_{max}, (g)	1.02	0.64
Energy spent to t_{max}, E_{max}, (KJ)	99.7	47
Maximum bed temperature at C_{max}, (^{O}C)	77	80
Time of 50% regeneration, (min)	26.17	16
Concentration at 50% regeneration $t_{50\%}$, (min)	3.43	3.3
Total mass regenerated, (g)	5.34	4.99
Energy spent to $t_{50\%}$, $E_{50\%}$, (KJ)	176.4	110
Maximum temperature measured at $t_{50\%}$, (^{O}C)	77.6	115
Carrier gas flow rate, slpm	1	1

Water vapor leaves the fixed bed earlier than toluene, removing an appreciable amount of energy that is deposited into the adsorber. Another possible issue that should be addressed for further desorption tests with adsorbed H_2O is that steam may contribute to polymerization reactions on the surface of carbon adsorbents. This type of reaction is usually caused by the breakdown of some adsorbates on the carbon surface in the presence of steam, air, or transitional metals from the electrodes used for electrothermal regeneration of the adsorbent (McInnes 1995).

Condensation Experimental Results

Previous experimental results for acetone and MEK indicated that the cryogenic condenser can be efficiently used to recover concentrated acetone and MEK vapors (Lordgooei et al. 1996; USEPA 1995). Figure 21 shows the effect of the condenser's influent vapor concentration on the condenser's theoretical LN_2 requirement. The LN_2 requirement is described as the mass of LN_2 consumed per unit mass of liquid VOC recovered. Higher condenser inlet vapor concentrations result in lower LN_2 consumption per unit mass VOC recovered up to about 10 percent by volume VOC. Such result indicates that the optimum vapor concentration during desorption should be about 10 percent by volume for undersaturated vapor concentrations. However, the overall energy efficiency can be increased appreciably by regenerating the VOC at supersaturated conditions. Figure 21 indicates that the mass of LN_2 required per unit mass of toluene and MEK recovered are almost the same, but are more than the amount of LN_2 required per unit mass of acetone recovered at the same inlet and outlet condenser temperatures.

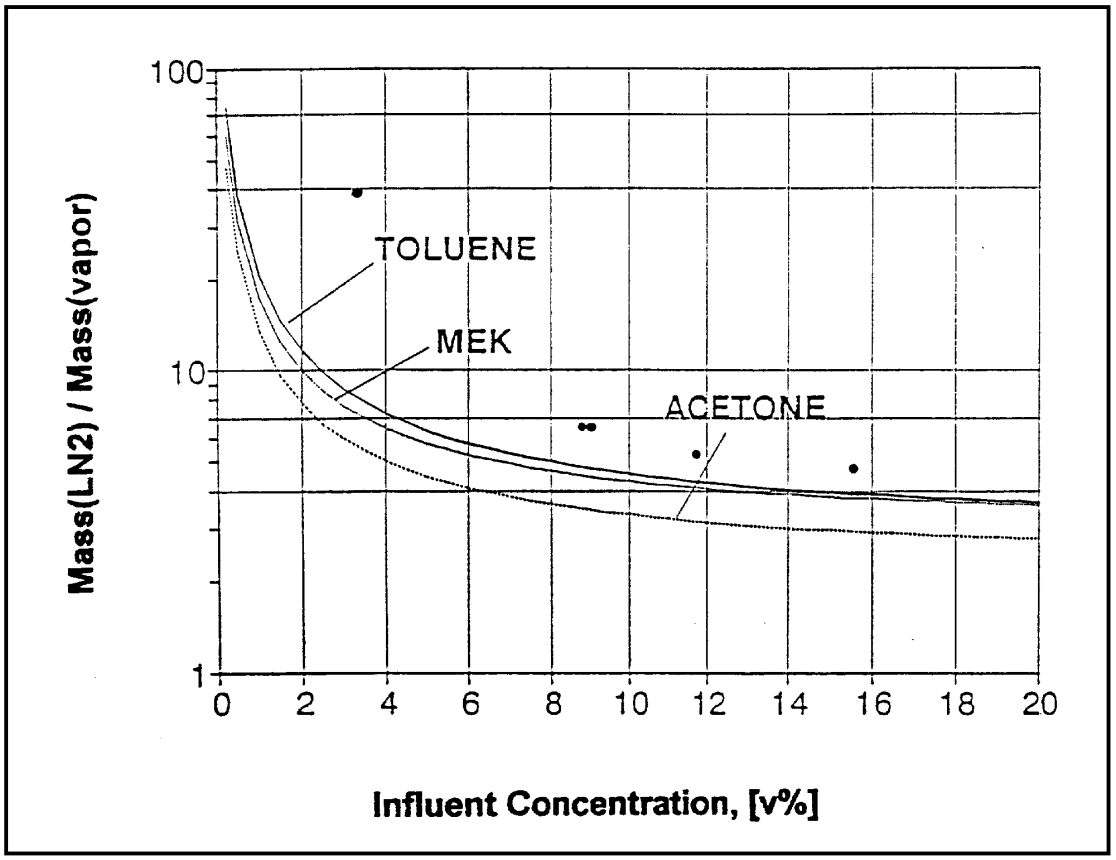

Figure 21. Condenser LN_2 consumption vs. TVOC concentration.

Figure 22 shows the dependence of MEK, toluene, and acetone saturation concentrations on temperature at a total pressure of 1 atm, as predicted by Wagner equation (Reed et al. 1987):

$$\ln\frac{P_v}{P_c} = \frac{V_{PA}x + V_{PB}x^{1.5} + V_{PC}x^3 + V_{PD}x^6}{1-x} \qquad \text{Eq 8}$$

where:

x = $1 - T/T_c$

P_v = vapor pressure (bar)

P_c = critical pressure (bar)

T_c = critical temperature (K)

T = temperature (K)

V_{PA}, V_{PB}, V_{PC}, and V_{PD} = constants.

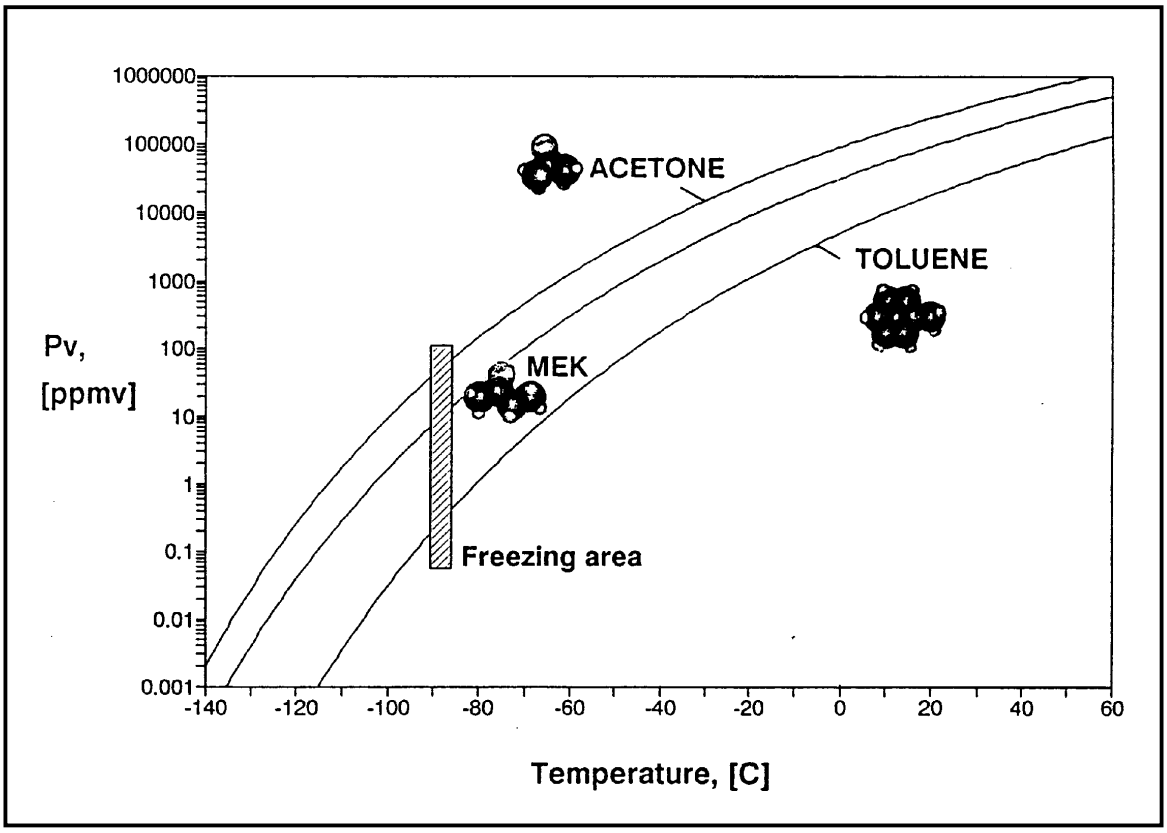

Figure 22. TVOC saturation concentration vs. equilibrium temperature at atmospheric total pressure.

Table 11 gives the related constants for acetone, MEK, and toluene. Figures 23 and 24 give the inlet and outlet acetone and MEK concentration as a function of log-mean condenser temperature. This profile shows that the condenser can operate close to modeled conditions using the Wagner equation to describe the saturated vapor concentration of the VOC.

Table 11. Experimental constants for use in the Wagner equation.

	Acetone	Toluene	MEK
Pc (bar)	47.0	41.0	42.1
Tc (K)	508.1	591.8	536.8
VP_A	-7.45514	-7.28607	-7.71476
VP_B	1.20200	1.38091	1.71061
VP_C	-2.43926	-2.83433	-3.68770
VP_D	-3.35590	-2.79168	-0.75169
*Source: Reid, R.C., Prausnitz, J.M., Poling, B.E., *The Properties of Gases and Liquids* 4th Ed., (McGraw Hill, 1987).			

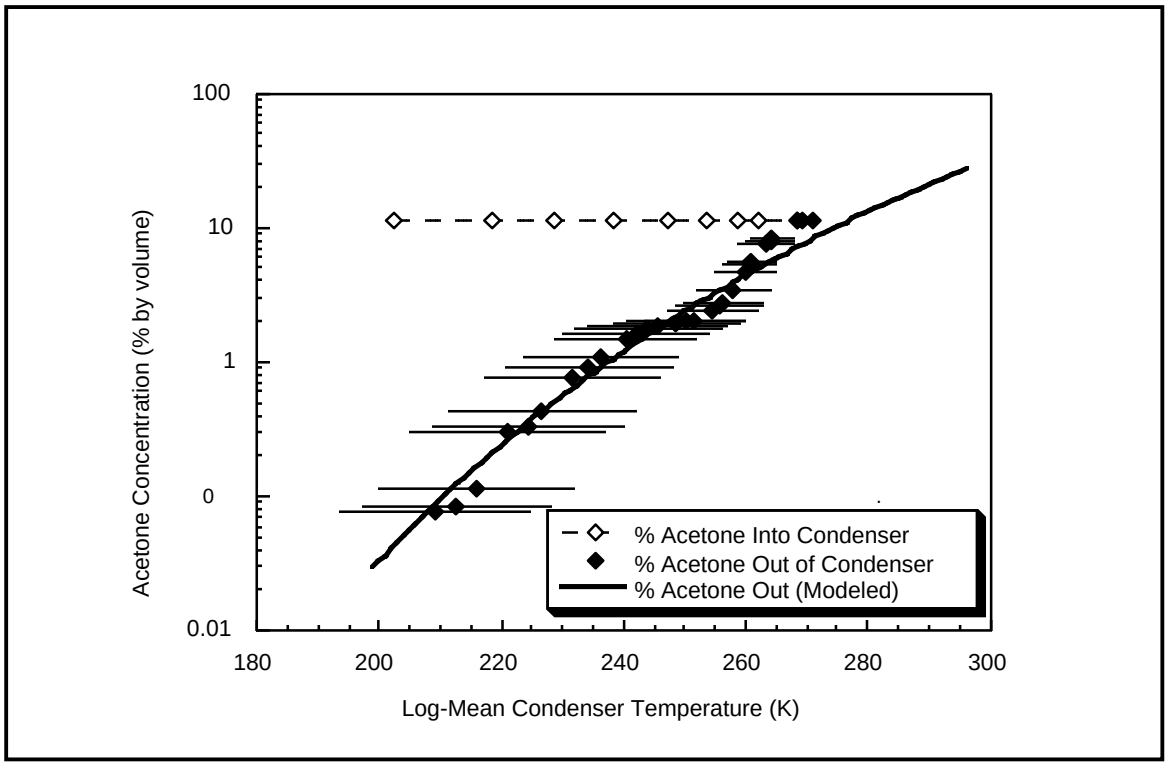

Figure 23. Inlet and outlet acetone concentrations vs. condenser temperature.

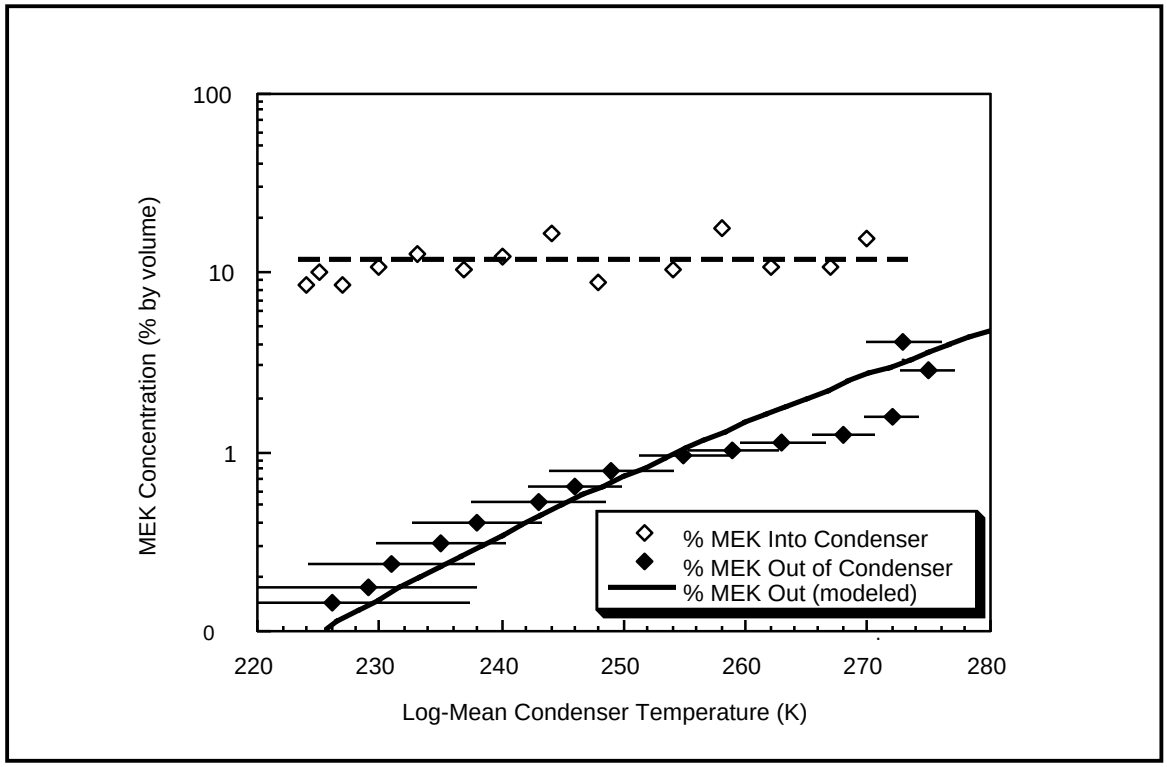

Figure 24. Inlet and outlet MEK concentrations vs. condenser temperature.

Test results for MEK condensation with the cryogenic condenser are given in Figure 25. The condenser is quite efficient in reducing MEK's concentration to very low values. Ambient temperature and pressure were 295 K and 746 mm Hg, respectively, during the tests. The total gas flow into the condenser is 0.5 alpm using the dual-bubbler gas generation system. The challenge stream was sent directly to the condenser operating at near steady-state temperature conditions. Outlet MEK concentrations remained near 1 percent by volume for simulated desorption inlet concentrations ranging from 23.8 to 1.5 percent by volume. The condenser mass removal efficiency was found to be 93.3 percent. Condenser response to a relatively high flow challenge gas stream was also evaluated. A 3.0 alpm MEK/N_2 challenge gas stream was sent into the condenser at near steady-state temperature conditions. Condenser outlet MEK concentrations ranged from 0.92 to 0.12 percent by volume for inlet concentrations ranging from 5.5 to 1.6 percent by volume. The achieved mass removal efficiency was 85.4 percent. The difference in removal efficiency is attributed to lower contact time and lower inlet MEK concentrations for the high flow MEK case.

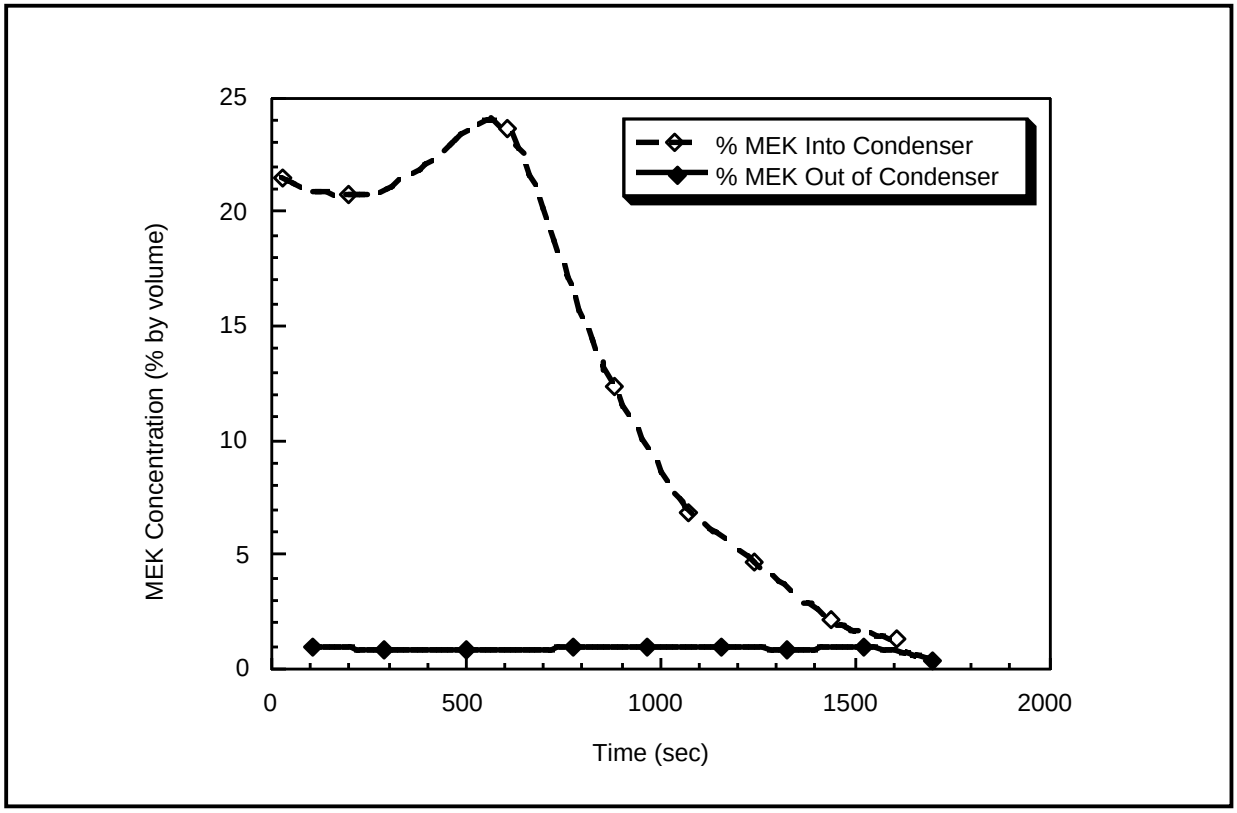

Figure 25. Condenser inlet and outlet MEK concentrations.

Cryogenic condensation of toluene was also performed in an integrated test with the ACFC fixed bed integrated with the condenser. This test was to evaluate the condenser outlet concentrations when desorbed toluene from the fixed bed adsorber is passed through the condenser. After the adsorption bed was saturated, the toluene was desorbed in a 1.1 slpm N_2 carrier stream using electrothermal regeneration. The desorbed gas stream was sent directly to the pre-cooled condenser at ambient temperature and ambient total pressure. Figure 26 shows temperature profiles from the condenser inlet and outlet. The initial part of the profile shows cool-down before any TVOC-laden gas stream was sent through the condenser. The temperature setpoint for the solenoid valve controlling LN_2 flow was 233 K. This temperature was reached after 50 minutes of condenser cool-down, at which point the desorbed gas stream was condensed. Figure 27 shows inlet and outlet TVOC concentration data for the gas stream as it passed through the condenser during desorption of the single component toluene experiment (test number 3C). The condenser's outlet toluene concentration exceeded 2,000 ppmv only once, even when the toluene inlet concentration of the gas stream entering the system was more than 30,000 ppmv. The condenser recovery efficiency was 97 percent over the 100-minute test.

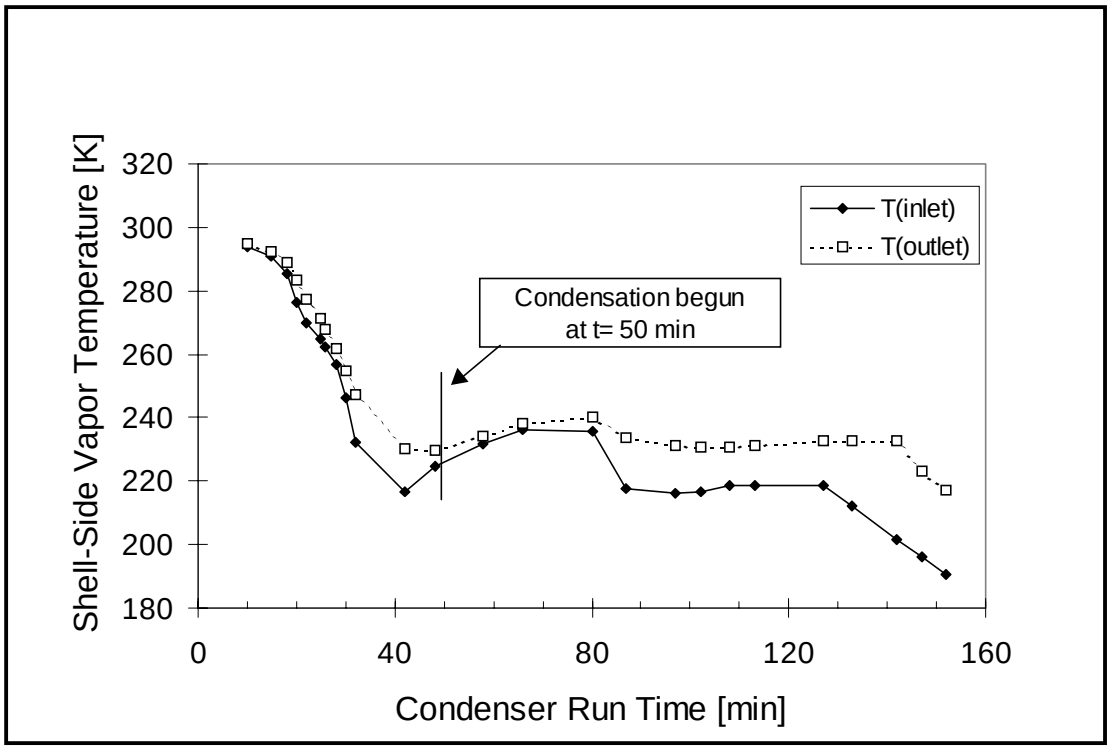

Figure 26. Condenser temperature profile during cool-down and condensation of toluene.

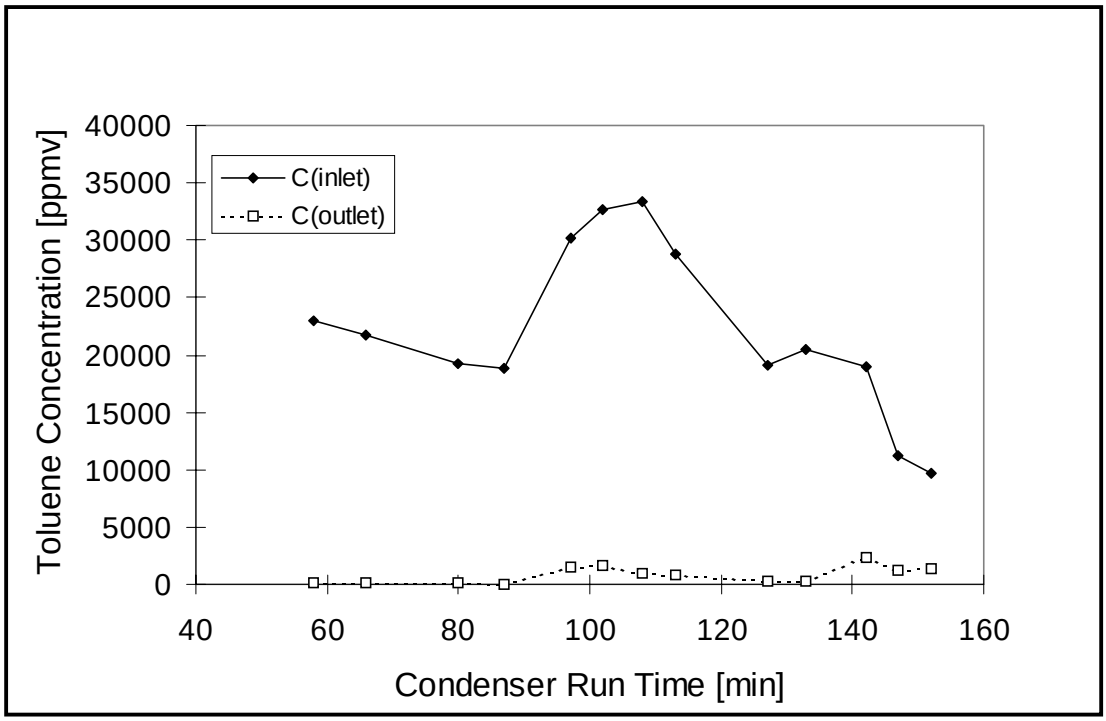

Figure 27. Condenser inlet and outlet toluene concentrations.

Figures 28 and 29, respectively, show GC/MS spectra from injections of liquid toluene from the bubblers and from the Erlenmeyer flask of recovered condensate. The sample size of liquid injected to the GC/MS was not the same for both of these spectra, with the sample of condensate being nearly three times as large as the toluene sample taken from the liquid toluene in the bubbler. The difference in sample size has altered the scale for the abundance, so that it may at first appear that more impurities existed in the bubbler than in the recovered toluene. The magnitude of impurities is more likely identical for the two samples, with only the particular mass/charge ratios of the impure compounds varying. Such results are encouraging because they suggest minimal (if any) change in the adsorbate during adsorption, desorption, and condensation. The second phase of the research project must more thoroughly evaluate and analyze the initial TVOC and its resulting condensate.

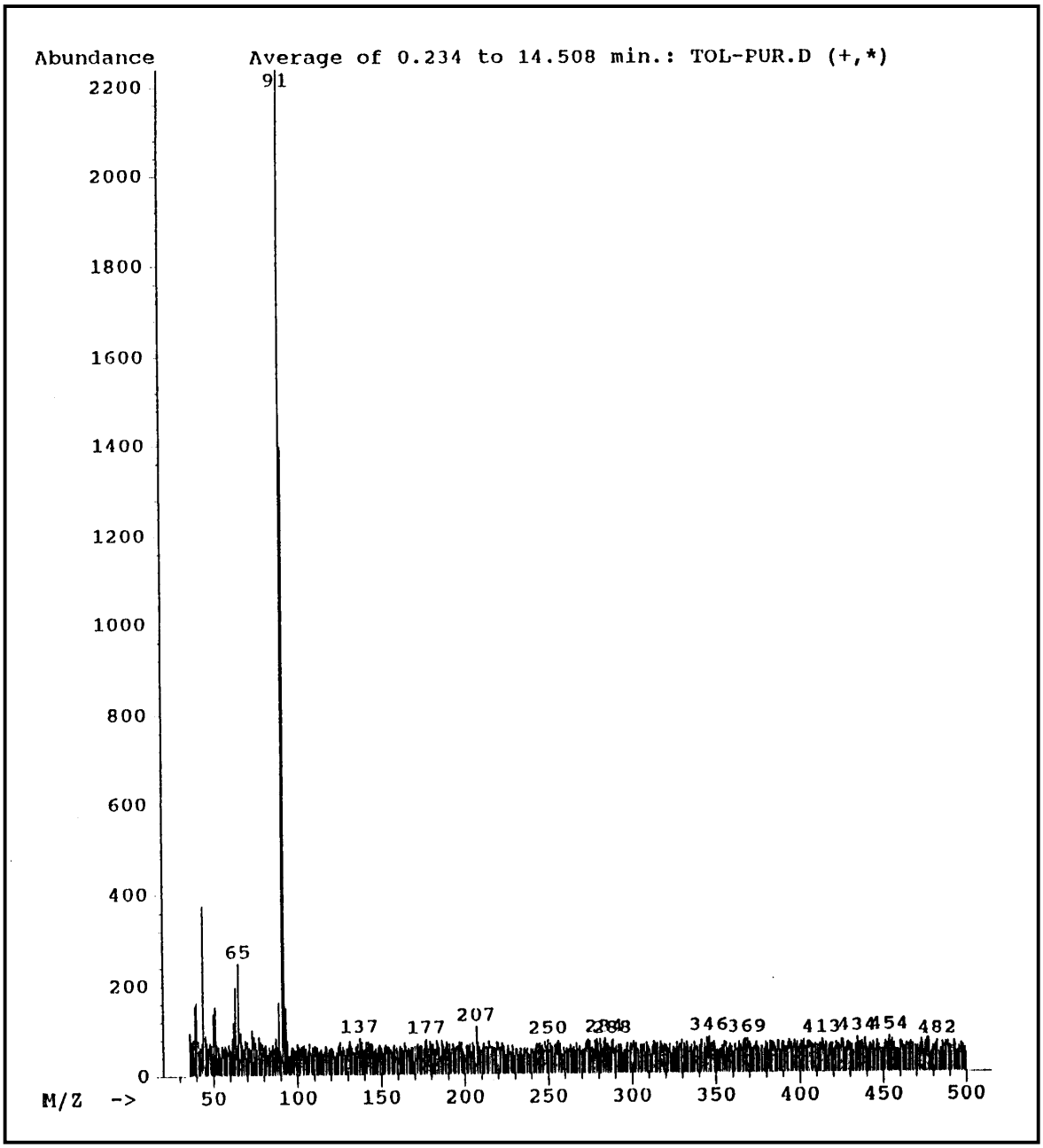

Figure 28. GC/MS spectrum for purity analysis of bubbler toluene.

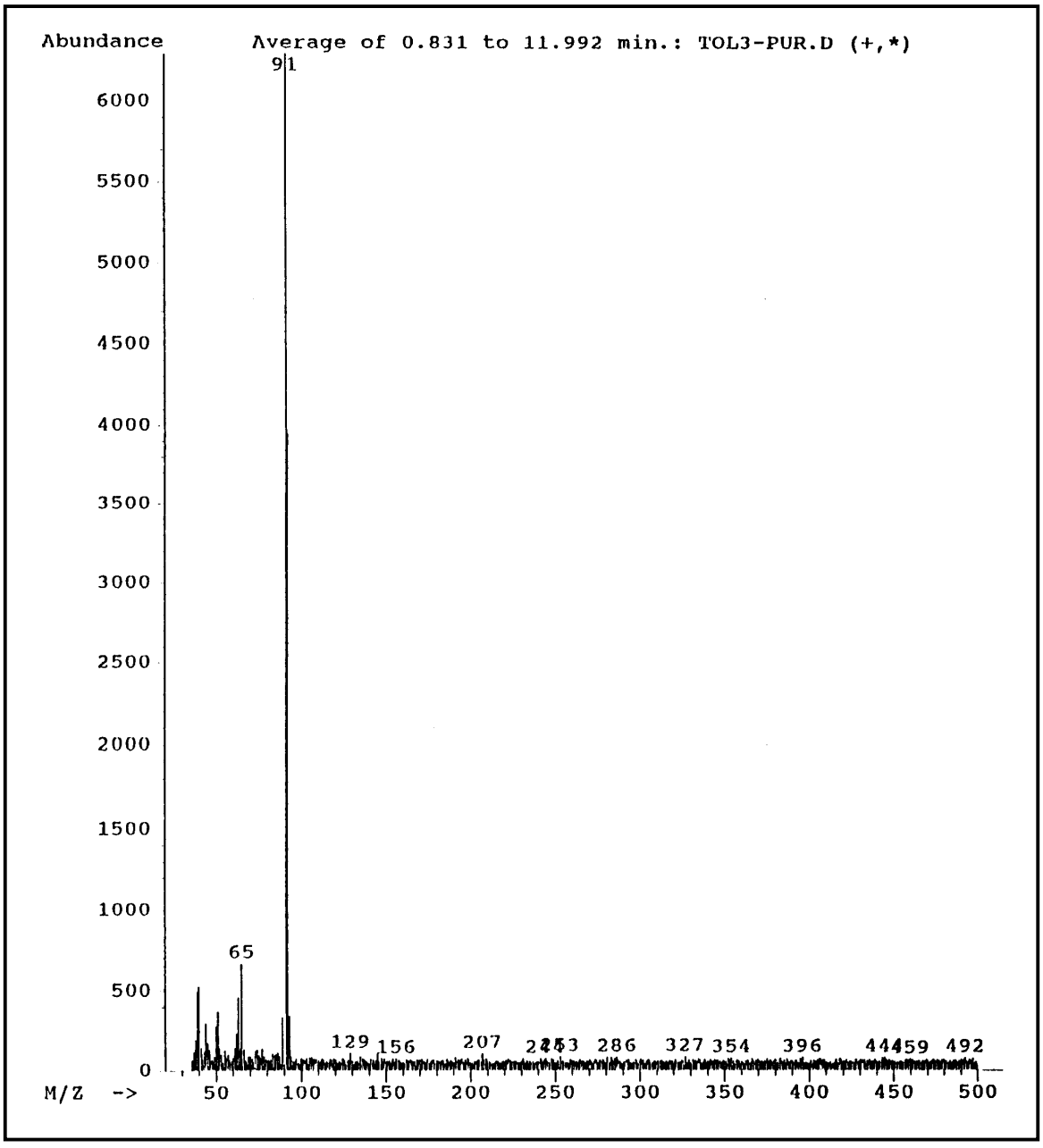

Figure 29. GC/MS spectrum for purity analysis of condenser-recovered toluene.

4 Cost Estimates

The overall electrothermal swing sorption system for capture and recovery of MEK or toluene includes the adsorption, electrothermal desorption, and condensation. The system is composed of two electrothermal ACFC adsorbers and one LN_2 condenser. During the adsorption cycle, the air stream containing 1000 ppmv of TVOC passes through an ACFC fixed-bed adsorber where ACFC separates MEK or toluene by adsorption. The clean air stream is then recycled or vented to the atmosphere. Just before breakthrough of MEK or toluene from the fixed bed, the untreated MEK and toluene stream is directed to the second bed to allow for continuous process operation while the exhausted bed is switched for electrothermal regeneration. During regeneration, an order of magnitude lower flow rate of N_2 gas is passed through the adsorption bed, and electrical power is supplied to the ACFC. Electrothermal energy regenerates the ACFC and provides an N_2 carrier gas stream containing the desorbed and concentrated MEK or toluene. The resulting MEK or toluene concentration in the N_2 carrier gas is controlled by the amount of electrical power supplied to the adsorbent and the flow rate and temperature of the carrier gas. The concentrated vapor stream is then directed to the condenser where the TVOC is condensed and separated from the N_2 carrier gas. The N_2 gas emitted from the condenser can then be used to cool the adsorber after the desorption step or vented to the atmosphere.

Table 12 itemizes costs for the electrothermal swing sorption system to recover 1,000 ppmv of MEK or toluene from a 10 m^3/min dry air stream. The preliminary calculations assume that the average concentration of the TVOC emitted from the adsorption bed during desorption is 10 percent by volume. Results of the adsorption and desorption experiments were used to estimate capital and annual cost of the electrothermal adsorber. To estimate the capital and annual cost of the condenser, factors were calculated using Figures 21-22 to determine the required ratio of LN_2 consumed per unit mass of MEK or toluene when compared to acetone. The detailed cost calculations for acetone condensation were available (Lordgooei et al. 1996). The two calculated factors applied to the cost to condense acetone and were then used to estimate costs to condense MEK and toluene.

For capture and recovery of MEK, the total annual cost for the system is $56,328/yr. Such cost compares favorably with the annual MEK recovery credit is $222,998/yr at $14.2/kg from GFC Chemicals Inc. The same type of economic analysis for capture and recovery of toluene resulted in a total annual cost for the system of $59,051/yr. Such does not compare as favorably to the annual toluene recovery credit of $4,742/yr. The cost of toluene is $0.24/kg compared to $14.2/kg for MEK. Such preliminary economic analyses indicate that toluene recovery by condensation is not a viable economic option. The high concentration of toluene generated by the electrothermal sorption process can be provided as the fuel for the process heaters or boilers. Therefore, for control of toluene at an initial concentration of 1,000 ppmv, an electrothermal sorption process might instead be considered as a preconcentrator for a combustion device. A separate study can show how concentration process can affect the cost of removal.

Cost information for a conventional thermal swing adsorption system is included in Table 12 to compare costs for an electrothermal swing adsorption system. Both systems treat a gas stream containing toluene under similar conditions. The thermal swing adsorption system consists of two steam regenerative adsorbers using commercially available Calgon BPL granular activated carbon, one cooling water condenser, and one decanter. Such system is not suitable for gas streams containing ketones. As previously mentioned, ketones can polymerize on the surface of many conventional carbonaceous adsorbents in the presence of metals that exist in the adsorbent's ash. The operating cycle times are the same for both systems. A larger amount of granular activated carbon is needed due to its lower adsorption capacity of toluene compared to ACFC. Adsorption capacity for a 1,000 ppmv toluene gas stream by Calgon BPL was estimated as 0.346 g/g-carbon (USEPA 1991). The thermal swing adsorption system requires three times more adsorbent and 2.4 times more volume than needed for the electrothermal swing adsorption system containing ACFC. The estimated total capital cost of the thermal swing adsorption system is $55,976 when using USEPA cost factors (USEPA 1991). This cost is 1.7 times higher than the estimated capital cost for the electrothermal swing adsorption system. The estimated annual operating cost of the thermal swing adsorption system, without considering costs to separate the recovered toluene from water and disposal of the condensate mixture, is $58,865. This cost is comparable with the annual cost of the electrothermal swing adsorption system.

Table 12. Economic analysis of the ACFC electrothermal swing and GAC thermal swing sorption system.

Adsorption system	Electrothermal Swing Adsorption	Electrothermal Swing Adsorption	Thermal Swing Adsorption
Number of adsorbers	2	2	2
Type of toxic volatile organic chemical	MEK in dry air	Toluene in dry air	Toluene in dry air
Molecular weight of the toxic gas	72	92	92
Density of liquid TVOC, g/cc	0.7994	0.8647	0.8647
Flow rate, Q (m^3/min)	10	10	10
Inlet adsorber temperature (K)	294	294	294
Bed operating Pressure, Pa	101325	101325	101325
Inlet adsorber concentration (ppmv)	1000	1000	1000
Inlet adsorber concentration (g/m^3)	2.985	3.814	3.814
Superficial gas velocity (cm/s)	20	20	80
Packing density (mg/cm^3)	300	300	400
Desired cross sectional area of fixed bed (cm^2)	8333	8333	2083
Form of the bed cross section	square	square	circular
Desired width or radius of the fixed bed (cm)	91.3	91.3	25.8
Selected width or radius of the fixed bed (cm)	90	90	26
Cross section of the fixed bed (cm^2)	8100	8100	2123
Fixed bed throughput ratio (%)	50	50	50
Breakthrough time (hr)	5.3	8.3	8.3
Stoichiometric time (hr)	10.6	16.6	16.6
Mass of adsorption till breakthrough (Kg)	9.491	18.992	18.992
Mass rate of TVOC recovered	1.791	2.288	2.288

Adsorption system (Kg/hr)	**Electrothermal Swing Adsorption**	**Electrothermal Swing Adsorption**		**Thermal Swing Adsorption**
Required bed adsorption equilibrium capacity (Kg)	18.982	37.985		37.985
ACC-5092-20 adsorption equilibrium capacity (g/g)	0.6	1.1	Calgon BPL GAC, g/g-C	0.346
Mass of ACC-5092-20 required per each bed, Kg	31.6372	34.5314	Calgon BPL GAC, Kg	109.78
Total mass of ACC-5092-20 required, Creq, Kg	63.2743	69.0627	Total mass of GAC	219.56
Volume of each fixed bed required (cm^3)	105457	115105		274454.49
Length of the fixed bed required (cm)	13.0194	14.2104		129.3
Selected bed length (cm)	13	14.2		130
Approximate adsorber vessel surface area (cm^2)	7020	7668		29716.96
Estimated vessel cost (Cv), Fall 1989 $	1307.05	1399.99		4016.42
Price of adsorbent $ per Kg.	20	20		2
Total cost of adsorbent, Cc ($)	1265.49	1381.25		
Auxilary equipment cost factor (Rc)	2.66718	2.66718		2.67
Adsorber cost, Fall 1989 $	10347.6	11152.1		22596.29
Regeneration Electrical Energy (KJ/g)	15	15	Regen. steam Kg/Kg-toluene	4
Time of electrothermal regeneration (hr)	0.5	1	Time of steam regeneration	1
Cooling time (hr)	4.8	7.3	Cooling time, hr	7.3
Total cycle time (hr)	10.6	16.6	Total Cycle Time, hr	16.6
Regeneration electrical cost per cycle (KW/Kg)	3.1	3.1	Superheat Steam cost, $/Tn	15

Adsorption system	Electrothermal Swing Adsorption	Electrothermal Swing Adsorption		Thermal Swing Adsorption
Regeneration electrical energy per cycle (KWh)	49.4	107.9	Regen. steam, $/cycle	1.1
Regeneration electrical annual cost (10 cents/KWh), $	4085	5695	Total cost of steam, $/yr	601.3
Total mass of adsorbate recovered per cycle (Kg)	9.5	19	Average Electrical requirement KW/Kcfm	6
Approximate annual cost of liquid nitrogen, $	10301	6689	Annual electricity cost, (0.1 $/KWh), $/yr	3153.6
Capital cost of condenser	13092	8501	Cooling water requirement, L/Kg-steam	100
			Total cooling water per cycle, L	7597
Direct Costs of Adsorber			Cooling water cost, $/m^3	0.05
Equipment Costs (Adsorber and auxiliary equipment), (EC) $	10347.6	11152.1	Cooling water cost, $/yr	200
Taxes for adsorber and auxiliary equipment (3% EC), $	310.427	334.563	Condenser cost (including pump,	
Freight (5% EC), $	517.378	557.605	Heat exchanger, decanter and auxil.), $	7000
Purchased Equipment Cost (PEC), $	11175.4	12044.3	Capital recovery factor for carbon	0.2638
			Carbon replacement cost, $	128
			Approximate cost of condensation, $/yr	6689
			Direct Costs of Adsorber	
			Equipment Costs (Adsorber	
			And auxiliary equipment), (EC) $	22596
			Taxes for adsorber and auxiliary	

Adsorption system	Electrothermal Swing Adsorption		Electrothermal Swing Adsorption	Thermal Swing Adsorption
			Equipment (3% EC), $	678
			Freight (5% EC), $	1130
			Purchased Equipment Cost (PEC), $	24532
Installation Direct Costs of Adsorber				
Structural supports (8% PEC)	894	964		1963
Erection and handling (14% PEC)	1565	1686		3434
Installation electrical cost (4% PEC)	447	482		981
Piping, installation, and painting (4% PEC)	447	482		981
Total Installed Direct Cost (30% PEC), $	3353	3613		7360
Total Direct Cost of Adsorber (DC), $	14528	15658		31892
Indirect Costs of Adsorber				
Engineering and supervision (10% PEC)	1118	1204		2453
Construction, field expenses, and fee (15% PEC)	1676	1807		3680
Start-up and performance test (3% PEC)	335	361		736
Contingency (3% PEC)	335	361		736
Total Indirect Costs of Adsorber, (IC)	3464	3734		7605
Total Capital Cost (TCC) of Adsorber, 1989 $	17992	19391		39497
CPI 1991-97	1.24	1.24		1.24
Total Capital Cost (TCC) of Adsorber, 1997 $	22311	24045		48976
Direct Annual Cost of Adsorber				

Adsorption system (DAC)	**Electrothermal Swing Adsorption**		**Electrothermal Swing Adsorption**	**Thermal Swing Adsorption**
Utilities:				
Electrical cost of regeneration, $	3358	9361	Utility cost of regeneration, $	3955
Operating:				
Labor (hrs/shift)	1	1		1
Operating labor ($/hr)	14	14		14
Annual labor hour	1095	1095		1095
Annual labor cost, $	15330	15330		15330
Supervisory Labor (15% of operator labor)	2300	2300		2300
Total operating cost of adsorber	17630	17630		17630
Maintenance:				
Labor ($14.5/hr)	3176	3176		3176
Materials (100% of maintenance labor)	3176	3176		3176
Total maintenance cost of adsorber	6351	6351		6351
Total DAC of adsorber	27338	33341		27936
Total DAC of the system including condenser and adsorber	37639	40030		34625
Indirect Annual Costs of Adsorber (IAC)				
Overhead, 0.6 (operating + maintenance)	14388	14388		14388
Property tax (1% of TCC)	223	240		490
Insurance (1% of TCC)	223	240		490
Adminstrative (2% of TCC)	446	481		980
Interest rate (%)	10	10		10
System life time, yrs	10	10		10
Capital Recovery Factor (CRF)	0.16	0.16		0.16

Adsorption system	Electrothermal Swing Adsorption	Electrothermal Swing Adsorption	Thermal Swing Adsorption
Capital recovery, CRF * (TCC - 0.025 (Creq) - 1.08 (Cc))	3408	3670	7892
Total annual costs of adsorber (IAC), $	18689	19020	24240
Total annual costs of the system, 1997 $	56328	59051	58865*
Total capital cost of the system, TCC $	35403	32546	55976
Annual TVOC recovery, Kg	15687	20045	20045
Price of TVOC, $/gallon	50	0.9	0.9
Price of TVOC, $/kg	14.2	0.2	0.2
Total annual solvent recovery credits, $	222998	4742	4742

*Annual cost of Separation of Toluene from water or disposal of the condensate mixture has not been included

5 Conclusions and Recommendations

This project has provided preliminary technical and economic evaluations of an activated carbon fiber cloth (ACFC) adsorption, electrothermal desorption, cryogenic-condensation system to remove 1000 ppmv methyl ethyl ketone (MEK) and toluene from air streams that are dry or at 90 percent relative humidity (RH).

Technical results indicate that MEK and toluene are readily adsorbed from air streams at low and high RH conditions with the ACFC fixed-bed adsorber. Electrothermal desorption is also effective at desorbing the TVOCs and water from the ACFC. Cryogenic condensation is also effective for the dry MEK and toluene adsorption cases.

Preliminary economic analyses for a 10 m^3/min dry air stream containing 1000 ppmv of MEK indicates a total annual cost for the air quality control system of $56,328/yr. The annual MEK recovery credit is $222,998/yr (four times greater than the annual cost). The same type of economic analysis for a 10 m^3/min dry air stream containing 1000 ppmv of toluene provided a total annual cost for the system of $59,051/yr. The annual toluene recovery credit is $4,472/yr.

Recommendations for additional laboratory development of the system during phase 2 of this research project include:

1. Implementation of new electrically insulated side walls for the adsorber or to redesign of the orientation of the ACFC near the walls of the bed to minimize localized heating and possible melting of the adsorber's internal walls

2. Operating the adsorber at elevated dry bulb temperatures for RH conditions to minimize the amount of water that adsorbs and then desorbs during electrothermal regeneration of the ACFC and therefore minimize problems related to water freezing in the condenser

3. Completion of careful material balances during adsorption and desorption cycles to explain discrepancies in the adsorption capacities of the adsorbent and the amounts of adsorbate that adsorbs and desorbs from the bed

4. Careful evaluation of the algorithm and setpoints used for the electrothermal desorption system

5. Construction and operation of a completely automated laboratory-scale ACFC electrothermal swing sorption system on a continuous basis for at least a 2-week period to optimize operating conditions for full-scale applications.

References

Burge, H.A., and M. Hodgson, "Health Risks of Indoor Pollutants," *ASHRAE J.*, vol 94, No. 7 (1988), pp 34-38.

Cal, M.P., *Characterization of Gas Phase Adsorption Capacity of Untreated and Chemically Treated Activated Carbon Cloths*, Ph.D. Thesis (University of Illinois at Urbana-Champaign [UIUC], 1995), p 3.

Cal, M.P., M.J. Rood, and S.M. Larson, "Gas Phase Adsorption of Volatile Organic Compounds and Water Vapor on Activated Carbon Cloth," *Energy & Fuels*, vol 11, No. 2 (1997), pp 311-315.

Carmichael, K.R., *Cryogenic Recovery of Volatile Organic Compounds for Re-Use*, Master's Thesis (UIUC, 1996).

Dyer, J.A., and K. Mulholland "Toxic Air Emissions: What is the Full Cost to Your Business," *Chemical Engineering*, vol 101, No. 2 (1994), pp 4-8.

Koloutsou-Vakakis, S., *Aerosol Particle Light Scattering at a Perturbed Mid-Latitude Continental Northern Hemispheric Site and its Dependence on Relative Humidity, Wavelength of Light, Particle Size, and Composition*, Ph.D. Dissertation (UIUC, 1996).

Lordgooei, M., K. Carmichael, M. Rood, and S.M. Larson, "Activated Carbon Cloth Adsorption-Cryogenic System To Recover Toxic Volatile Organic Compounds," *Gas. Sep. Purif.*, vol 10, No. 2 (1996), pp 123-130.

Lordgooei, M., K.R. Carmichael, M.J. Rood, and S.M. Larson, *Development of an Activated Carbon Fiber Cloth Adsorption/Regeneration System To Recover and Reuse Toxic Organic Compounds*, Draft Report HWR94115 (Hazardous Waste Research and Information Center, 1996).

Marcus, Y., "Principles of Solubility and Solutions," *Principles and Practices of Solvent Extraction*, Ryberg et al., eds. (Marcel Dekker, Inc., 1992), p 23.

Mcllvaine, R., S. Halderman, and J. Schwartz, "Can Air Toxics and VOC Reduction Goals Be Met," *Pollution Engineering* (February 1993), pp 54-57.

McInnes, R.G., "Explore New Options for Hazardous Air Pollutant Control," *Chemical Engineering Progress*, vol 91 (November 1995), pp 36-48.

Noll, K.E., V. Gounaris, and W.S. Hous, *Adsorption Technology for Air and Water Pollution Control*, (Lewis Publishers Inc., 1992).

Perry, R.H., and C.H. Chilton, *Chemical Engineer's Handbook*, 5th ed. (McGraw Hill, 1973), pp 3:38-3:43.

Reid, R.C., J.M. Prausnitz, B.E. Poling, *The Properties of Gases and Liquids*, 4th ed. (McGraw Hill, 1987).

Ruddy, E.N., and L.A. Carrol, "Select the Best VOC Control Strategy," *Chemical Engineering Progress* (July 1993), pp 28-35.

Tolley, G., J. Wentz, S. Hilton, and B. Edwards, *The Urban Ozone Abatement Problem, Cost Effective Control of Urban Smog*, Conference proceedings from workshop on market-based approaches to environmental policy (1993), pp 9-28.

U.S. Environmental Protection Agency (USEPA), Clean Air Act Amendments (USEPA, 1990).

USEPA, *Control Technologies for Hazardous Air Pollutants*, EPA/625/6-91/014 (USEPA, 1991).

USEPA, *Control Technology Guideline Series: Control of Volatile Organic Compound Emissions from Reactor Processes and Distillation Operation Processes in the Synthetic Organic Chemical Manufacturing Industry*, prepared for USEPA under purchase order No. EPA-450/4-91-031 (1991).

USEPA, *National Air Quality and Emissions Trends*, EPA/454/R-93-03 (USEPA, 1993).

USEPA, *1991 Toxics Release Inventory* (USEPA, 1993).

USEPA, *1993 Toxics Release Inventory, Executive Summary*, Catalog No. PA745595001 (USEPA, 1995).

USEPA, *Control Technologies for Hazardous Air Pollutants*, Summary Catalog No. PA-625/6-91/014 (USEPA, 1991).

CERL DISTRIBUTION

Chief of Engineers
ATTN: CEHEC-IM-LH (2)
ATTN: CEHEC-IM-LP (2)
ATTN: CECG
ATTN: CECC-P
ATTN: CECC-R
ATTN: CECW
ATTN: CECW-O
ATTN: CECW-P
ATTN: CECW-PR
ATTN: CEMP
ATTN: CEMP-E
ATTN: CEMP-C
ATTN: CEMP-M
ATTN: CEMP-R
ATTN: CERD-C
ATTN: CERD-ZA
ATTN: CERD-L
ATTN: CERD-M (2)

HQIOC 61299-6000
ATTN: AMSIO-IBB-ENV

ACS(IM) 22060
ATTN: DAIM-FDP

CEISC 22310-3862
ATTN: CEISC-E
ATTN: CEISC-FT
ATTN: CEISC-ZC

US Army Engr District
ATTN: Library (40)

US Army Engr Division
ATTN: Library (8)

USA TACOM 48397-5000
ATTN: AMSTA-XE

Defense Distribution Region East
ATTN: ASCE-WI 17070-5001

US Army Materiel Command (AMC)
Alexandria, VA 22333-0001
ATTN: AMCEN-F
ATTN: AMXEN-C 61299-7190
Installations: (20)

FORSCOM
Forts Gillem & McPherson 30330
ATTN: FCEN
Installations: (20)

TRADOC
Fort Monroe 23651
ATTN: ATBO-G
Installations: (19)

Fort Belvoir 22060
ATTN: CETEC-IM-T
ATTN: Water Resources Support Ctr

USA Natick RD&E Center 01760
ATTN: STRNC-DT
ATTN: AMSSC-S-IMI

US Army Materials Tech Lab
ATTN: SLCMT-DPW 02172

CEWES 39180
ATTN: Library

CECRL 03755
ATTN: Library

USA AMCOM
ATTN: Facilities Engr 21719
ATTN: AMSMC-EH 61299
ATTN: Facilities Engr (3) 85613

USA Engr Activity, Capital Area
ATTN: Library 22211

US Army ARDEC 07806-5000
ATTN: AMSTA-AR-IMC

Linda Hall Library
ATTN: Receiving 64110-2498

Defense Logistics Agency
ATTN: DCSC-BI 22060-6221

US Military Academy 10996
ATTN: MAEN-A
ATTN: Facilities Engineer
ATTN: Geography & Envr Engrg

Naval Facilities Engr Command
ATTN: Facilities Engr Command (8)
ATTN: Engrg Field Divisions (10)
ATTN: Engrg Field Activities (4)
ATTN: Public Works Center (8)
ATTN: Naval Constr Battalion Ctr 93043
ATTN: Naval Facil. Engr. Service Ctr 93043-4328

Tyndall AFB 32403
ATTN: HQAFCESA/CES
ATTN: Engrg & Srvc Lab

American Public Works Assoc. 64104-1806

US Army CHPPM
ATTN: MCHB-DE 21010

US Gov't Printing Office 20401
ATTN: Rec Sec/Deposit Sec (2)

Nat'l Institute of Standards & Tech
ATTN: Library 20899

Defense Tech Info Center 22060-6218
ATTN: DTIC-O (2)